Published in final edited form as:
Neuroscience. 2010 December 15; 171(3): 893–909. doi:10.1016/j.neuroscience.2010.08.059.

Ovarian Steroid Regulation of the Midbrain CRF and UCN Systems in Macaques

Rachel L. Sanchez[1], **Arubala P. Reddy**[1], and **Cynthia L. Bethea**[1,2,3,4]

[1] Division of Reproductive Sciences, Oregon National Primate Research Center, Beaverton, OR 97006

[2] Division of Neuroscience, Oregon National Primate Research Center, Beaverton, OR 97006

[3] Department of Behavioral Neuroscience, Oregon Health and Science University, Portland, Oregon 97239

[4] Department of Obstetrics and Gynecology, Oregon Health and Science University, Portland, Oregon 97239

Abstract

A significant number of postmenopausal women report increased anxiety and vulnerablity to stress, which has been linked to decreased secretion of ovarian steroids. Communication between the serotonin system and the CRF system determines stress sensitivity or resilience. This study examines the effects of the ovarian steroids, estradiol (E) and progesterone (P) on the CRF system components that impact serotonin neurons in the midbrain of nonhuman primates. Ovariectomized rhesus macaques were treated with placebo, E alone for one month, or E supplemented with P for the last 2 weeks. Quantitative (q)RT-PCR and immunocytochemistry were employed. E±P treatment decreased CRF-R1 and increased CRF-R2 gene expression in hemi-midbrain blocks and in laser captured serotonin neurons. Also in hemi-midbrains, E treatment increased UCN1 and CRFBP gene expression, but supplemental P treatment reversed these effects. E±P suppressed the already very low UCN3 mRNA, but had no effect on UCN2 mRNA. E±P decreased CRF fiber density in the dorsal, interfascicular and median raphe nuclei and decreased CRF-R1 immunostaining in the dorsal raphe. E increased CRF-R2 immunostaining in the dorsal and median raphe. E±P increased UCN1 immunostaining in the cell bodies and increased UCN1 fiber density in the caudal linear nucleus. ERβ, but not ERα was detected in the nucleus of UCN1-positive neurons. While the mechanism of ovarian hormone regulation of the midbrain CRF system requires further investigation, these studies clearly demonstrate another pathway by which ovarian hormones may have positive effects on anxiety and mood regulation.

Keywords

serotonin; corticotropin; urocortin; estrogen; progesterone; macaques

Corresponding Author and to whom reprint requests should be directed: Cynthia L. Bethea, Ph.D., Tel 503-690-5327, Fax 503-690-5384, betheac@ohsu.edu.

Disclosure

The authors have no relevant financial interests to disclose.

Introduction

Women experience ovarian failure and loss of ovarian steroid production around 50 years of age. Thus, with extended life spans, a woman may live 35–40 years without ovarian steroids. After menopause, a significant number of women become more anxious, and less able to cope with stress, leading to new onset of depression (Maki et al., Conde et al., 2006, Heikkinen et al., 2006, Tangen and Mykletun, 2008). The role of ovarian hormones in depression and stress sensitivity is of great interest for women transitioning through menopause and questioning the use of hormone therapy.

The serotonin system plays a pivotal role in affective disorders, including depression and anxiety. The administration of selective serotonin reuptake inhibitors (SSRIs) is to date, the most effective pharmacological intervention for depression and anxiety disorders (Owens and Nemeroff, 1994). This laboratory has shown that the ovarian steroids, estrogen (E) and progesterone (P) increase serotonin neural function (Bethea et al., 2002) and protect serotonin neuronal health in monkeys (Bethea et al., 2009), which could translate to improved mood and stress resilience in women.

The hypothalamic-pituitary adrenal axis has also been implicated in the etiology of depression (Morimoto et al., 1993, Weiss et al., 1994, Nemeroff, 2004b), and a stress-induced elevation in corticotropin releasing factor (CRF) in the hypothalamic paraventricular nucleus (PVN) is thought to underlie the hyperactivity of the HPA axis in depression (Holsboer, 1999, Keck and Holsboer, 2001, de Kloet et al., 2005). We found that E or E+P *decrease* CRF gene and protein expression in the PVN of macaques (Bethea and Centeno, 2008), which could also translate to stress resilience.

The relationship between CRF signaling and serotonin transmission has attracted significant interest. There is a prominent serotonergic projection to the PVN (Petrov et al., 1992, Hanley and Van de Kar, 2003) where 5HT2A and 5HT2C receptors are robustly expressed in monkeys (Gundlah et al., 1999). There is also a reciprocal CRF projection from the PVN to the midbrain dorsal and median raphe nuclei, the location of serotonin neurons that project to the forebrain (Luiten et al., 1985, Portillo et al., 1998). In a human study, CRF fibers and terminals apposed serotonin cell bodies and primary dendrites in the raphe region (Ruggiero et al., 1999). In rodents, CRF-R1 and CRF-R2 receptors have been observed in the dorsal raphe nucleus and CRF has complex and opposing effects depending on the dose used and the endpoint examined (Pernar et al., 2004). However, information on the effect of ovarian steroids on the relationship between CRF and serotonin systems in the nonhuman primate brain is lacking.

The ‘CRF system’ is comprised of several related ligands and receptors. The ligands are CRF and the urocortins 1, 2 and 3 (UCN1, UCN2, UCN3). CRF and urocortins mediate their effects by activating two known G-protein coupled receptors, CRF-R1 and CRF-R2 (Dautzenberg and Hauger, 2002). CRF has a higher affinity for CRF-R1 than CRF-R2. In contrast, UCN1 binds CRF-R2 with higher affinity than it binds CRF-R1 (Vaughan et al., 1995). The distribution of the CRF-R1 and CRF-R2 receptors is distinct and implies diverse physiological functions, as evidenced by the divergent phenotypes of CRF-R1- and CRFR2-null mice (Smith et al., 1998, Timpl et al., 1998, Muller et al., 2003, Keck et al., 2005). It is thought that CRF-R1 mediates anxious behavior and the HPA axis response to stress, while CRF-R2 mediates stress-coping behaviors such as anxiolytic behaviors, dearousal, and cardioprotection (Valdez et al., 2002). Therefore, either inhibition of CRF-R1 and/or stimulation of CRF-R2 could decrease anxiety and related depressive behaviors. In addition, CRF and UCN1 also interact with binding proteins, CRFBP and sCRFR2α (Behan et al.,

1995b). Each binding protein binds CRF or UCN1 extracellularly and is thought to prevent receptor activation (Behan et al., 1995a, Kemp et al., 1998).

We questioned whether the steroid-induced decrease in CRF expression in the PVN (Bethea and Centeno, 2008) would be manifested in the CRF innervation of the dorsal and median raphe, and whether ovarian steroids regulate CRF receptors in raphe terminal fields in macaques. In addition, we determined the effect of E and P on midbrain urocortin, considered part of the CRF family of ligands. We used a primate model of surgical menopause with hormone treatment for one month.

Materials and Methods

The Institutional Animal Care and Use Committee of the Oregon National Primate Research Center (ONPRC) approved this study.

Animals

Adult female rhesus monkeys (Macaca mulatta) were ovariectomized (Ovx) by the surgical personnel of ONPRC according to accepted veterinary protocol, approximately 5 to 16 months before assignment to this project. All animals were born in China, were aged between 7–14 years, weighed between 4 and 8 kg, and were in good health. ONPRC operates with a lease for fee arrangement. Thus, the animals were previously used in select reproductive protocols in which ovariectomy was the final step before releasing the animals back into the available pool.

Animals were either treated with placebo (ovx-control group), or treated with estradiol (E) for 28 days (E group), or treated with E for 28 days and supplemented with progesterone (P) for the final 14 of the 28 days (E+P group). The placebo treatment of the ovx-control monkeys consisted of implantation with empty Silastic capsules (s.c.) on day 0 and day 14. The E-treated monkeys were implanted (s.c.) with one 4.5-cm E-filled Silastic capsule (i.d. 0.132 in.; o.d. 0.183 in.; Dow Corning, Midland, MI) on day 0 and an empty capsule on day 14. The E+P- treated group received an E-filled capsule, and 14 days later, received one 6-cm P capsule. All capsules were placed in the periscapular area under ketamine anesthesia (ketamine HCl, 10mg/kg, s.c; Fort Dodge Laboratories, Fort Dodge, IA).

The E capsule was filled with crystalline estradiol (1,3,5(10)-estratrien-3, 17-b-diol; Steraloids, Wilton, NH). The P capsule was filled with crystalline P (4-pregnen-3, 20 dione; Steraloids).

Fifteen animals were used for immunocytochemistry (n=5/group); twelve animals were used for qRT-PCR on hemi-midbrain blocks (n=4/group), and nine animals were used for laser capture of serotonin neurons and subsequent qRT-PCR (n=3/group). The average time (months) between ovariectomy and hormone treatment for each set of animals equaled 5.2±0.85, 7.2±1.0 and 16.2±5.3, respectively.

Euthanasia

The monkeys were euthanized at the end of the treatment periods according to procedures recommended by the Panel on Euthanasia of the American Veterinary Association. Each animal was sedated with ketamine in the home cage, transported to the necropsy suite, given an overdose of pentobarbital (25 mg/kg, i.v.), and exsanguinated by severance of the descending aorta.

Tissue preparation for immunocytochemistry

The left ventricle of the heart was cannulated and the head of each animal was perfused with 1 liter of saline followed by 7 liters of 4% paraformaldehyde in 3.8% borate, pH 9.5 (both solutions made with DEPC treated water [0.1% diethyl pyrocarbonate] to minimize RNase contamination). The brain was removed and dissected. Tissue blocks were post-fixed in 4% paraformaldehyde for 3 hours, then transferred to 0.02 M potassium phosphate-buffered saline (KPBS) containing 10%, followed by 20% glycerol and 2% dimethyl sulfoxide (DMSO) at 4C for 3 days to cryoprotect the tissue. After infiltration, the block was frozen in isopentene cooled to −55C, and stored at −80C until sectioning in the coronal plane, which occurred within 3 months of storage. Sections (25μm) were cut on a sliding microtome, collected in a cryoprotectant buffer (30% ethylene glycol and 20% glycerol in 0.05M PBS) and then frozen at −20° C until processed with immunocytochemistry.

Tissue preparation for qRT-PCR on the hemi-midbrain tissue block

The brain was perfused with saline, removed and dissected. The pontine midbrain was bisected along the midline (saggital plane). One side was immersed in 1X RNA later for one week at 4°C, and then frozen in aluminum foil at −80 °C until RNA extraction (gift of Dr. Henryk Urbanski).

Tissue preparation for laser capture of serotonin neurons

The brain of each animal was perfused with 3 liters of 1X cold RNA-later buffer (Ambion Inc., Austin, TX) plus 20% sucrose. The brain was removed from the cranium, dissected into blocks and frozen at −80°C until sectioning at 7 μm in the coronal plane and laser capture of serotonin neurons as previously published (Bethea and Reddy, 2008).

Immunocytochemistry

Brain sections were removed from frozen storage and washed in KPBS for an hour. They were blocked in the appropriate normal serum for an hour, and then blocked in avidin and biotin for 20 minutes (Vector labs, Burlingame, CA). The primary antibody was diluted in 0.02 M KPBS/2% normal rabbit or goat serum/0.4% Triton X-100 and exposed to the experimental tissue for 48 hours at 4°C. After 48h, sections were washed in KPBS for an hour. The appropriate secondary antibody (Vector) was diluted 1:200 in KPBS/0.4% triton and incubated with the tissue for 60 minutes. After another KPBS wash, the tissue sections were incubated in VECTASTAIN Elite ABC solution (Vector) for one hour and washed in buffer again. Sections were then incubated in 0.02M KPBS with 0.05% DAB and 0.003% H_2O_2. Finally, the sections were washed, mounted on slides, dehydrated, dipped in xylene, and then coverslipped in DPX mountant for stereological analysis.

The CRF antibody was a gift from Dr. Wylie Vale (Salk Institute, La Jolla, CA) and was raised in rabbit against human CRF conjugated to human alpha globulin. Thus, in the CRF ICC, we used an additional blocking step with 1% human alpha globulin (Sigma G-2011) for 20 minutes. Rabbit anti-human CRF (1/15,000) was diluted in 0.02 M KPBS/2% normal goat serum/0.4% triton/0.1% human alpha globulin. The secondary antibody was biotinylated goat anti-rabbit IgG (Vector). The antisera to CRF has been extensively characterized and previously applied to primate brain (Bassett and Foote, 1992).

The UCN1 antibody (Sigma-Aldrich, St. Louis, MO; Catalog No. U4757) was raised in rabbit against amino acids 25–40 of the human peptide. Prior to incubation with the primary antibody, an additional blocking step with 3% bovine serum albumin for an hour was included. Rabbit anti-UCN1 (1/15,000) was diluted in 0.02 M KPBS/2% normal goat serum/ 0.4% triton. The secondary antibody was biotinylated goat anti-rabbit IgG (Vector). The

antisera to UCN1 has been extensively characterized and previously applied to rat and human brain (May et al.).

The CRF-R1 antibody (Santa Cruz Biotechnology, Santa Cruz, CA; Catalog No. 12381) was an affinity purified goat polyclonal antibody raised against an internal region of CRF-R1 of human origin. Increasing dilutions of anti-CRF-R1 produced decreasing signal up to a titer of 1/4000, beyond which the signal disappeared. Anti-CRF-R1 was diluted 1/500 in 0.02 M KPBS/2% normal rabbit serum/0.4% triton and incubated with the experimental tissue for 48 hours at 4°C. The secondary antibody was biotinylated rabbit anti-goat IgG (Vector). As a further control, the highest titer of CRF-R1 antibody that detected signal (1/2000) was preabsorbed with a blocking peptide matched to the antibody (500 μg; Santa Cruz Biotechnology, Santa Cruz, CA; Catalog No. 12381-P) at 4°C overnight. The CRF-R1 antibody and the preabsorbed antibody were incubated on adjacent tissue sections for 48 hours at 4°C. Two days later, the tissue was incubated with secondary antibody and processed as described above.

The CRF-R2 antibody (Chemicon International, Billerica, MA; Catalog No. AB9139, lot 0602022158) was raised in rabbit against the first extracellular domain of human CRF-R2. Increasing dilutions of anti-CRF-R2 produced decreasing signal to background up to a titer of 1/2000. Anti-CRF-R2 was diluted 1/750 in 0.02 M KPBS/2% normal goat serum/0.4% triton and exposed to the experimental tissue for 48 hours at 4°C. The secondary antibody was biotinylated goat anti-rabbit IgG (Vector). As a further control, the CRF-R2 antibody at 1/750 was preabsorbed with the peptide used to make the antibody (1 mg; Lifespan Biosciences, Seattle, WA) at 4°C overnight. The CRF-R2 antibody and the preabsorbed antibody were incubated on adjacent tissue sections for 48 hours at 4°C. Two days later, the tissue was incubated with secondary antibody and processed as described above.

Double Immunocytochemistry

Localization of estrogen receptor beta (ERβ) and UCN1 in the $pIII_u$ was sought using double label IHC. Sections (25 μm) of the pIIIu were obtained from an extra monkey and stored in cyroprotectant at −20°C until the day of assay. For assay, sections were mounted on slides. The slides were washed in 0.02M KPBS, blocked in normal goat serum, avidin, and biotin, and incubated at 4°C overnight with anti-human ERβ IgG (mouse monoclonal, 1:100, Serotec). The next day, slides were washed in KPBS, incubated with biotinylated goat anti-mouse secondary antibody, and then washed again before incubation with ABC solution (Vector labs). A solution of 10 ml 0.05M Tris containing 395 g nickel ammonium sulfate, 7 mg diaminobenzidine (DAB; 0.07%), and 2 μL 30% hydrogen peroxide (0.006%) was prepared and 500 μl was placed onto the sections for 10 minutes. The antigen-antibody complex was visualized as a purple nuclear stain. This nuclear ERβ stain was fixed in 4% paraformaldehye/0.1M phosphate for one hour. This was followed by rinsing in 0.02 M KPBS and blocking with normal goat serum (NGS), avidin, and biotin. The slides were incubated at 4°C for 48 hours with rabbit anti-UCN1 polyclonal antiserum. Two days later, the slides were washed in KPBS, and then incubated with goat anti-rabbit biotinylated secondary antibody. After incubation with ABC solution, a solution of 0.02M KPBS containing 0.05% DAB and 0.003% hydrogen peroxide was prepared and 500 μl was placed onto the sections for 2 minutes. The reaction was terminated with a KPBS wash. Slides were vacuum dried overnight, dehydrated through a grades series of ethanol, dipped in xylene, and coverslipped in DPX mountant.

Stereological Analysis of Immunostaining

Sections were anatomically matched between animals using anatomical reference points. A Marianas Stereological workstation with Slidebook 4.1 was used for analysis. Each section

was examined and guidepoints demarcating the area of interest were entered. The workstation captured multiple 10x images across the span of the area and built a 10x montage of the entire area. The software then segmented the montage based upon signal density. The CRF and UCN1 positive fibers were highlighted and the highlighted area was quantified in pixels. Finally, the total area examined (region of interest) was obtained. For cell counting, the software allows the operator to mark each positive cell and tallies the total number of marked cells. The values were recorded and then subjected to further statistical analysis.

qRT-PCR on the midbrain tissue block

RNA was obtained from the microdissected hemi-midbrain block of 12 rhesus midbrains (previously infiltrated with RNA later) using TriReagent and further cleaned with a Qiagen RNAeasy column (Velencia, CA). The quality of the RNA from the Qiagen column was examined on an Agilent Bioanalyzer and found acceptable and of equal quality. The RNA was subjected to quantitative (q) RT-PCR for 6 genes of greatest interest, which were: CRF-R1, CRF-R2, CRF-Binding Protein (BP), UCN1, UCN2 and UCN3. Tryptophan hydroxylase 2 (TPH2) was also examined as a physiological control for E and P regulation of gene expression.

Complementary DNA (cDNA) synthesis was performed using Oligo-dT 15 primer and random hexamer (Invitrogen Life Technologies, Carlsbad, CA) and Superscript III reverse transcriptase (200 U/μg of RNA, Invitrogen Life Technologies) at 50°C for 1 hr. A pool of RNAs from different rhesus tissues was used as the standard.

Taqman qPCR array

Four different concentrations of cDNA from the pool of rhesus tissues (0.5, 5.0, 50.0, 500.0 ng) and 25 ng of the 12 hemi-midbrain samples (in 100 μl reaction mix) were loaded onto custom Taqman microfluidic PCR cards according to the manufactor s specifications (Applied Biosystems Inc., Foster City, CA; https://products.appliedbiosystems.com/ab/en/US/adirect/ab?cmd=catNavigate2&catID=601274). Thus, each reaction well contained about 1 ng of midbrain cDNA sample. The cards contained proprietary primer sets for amplification of rhesus CRF-R1, CRF-R2, CRFBP, UNC1, UCN2, UCN3, TPH2 and GAPDH. The ABI primer set identification numbers, context sequences and the NCBI gene reference numbers are listed in Table 1. Each standard concentration and sample was amplified in triplicate for each primer set. The 5 fluorescent reporter on the probe was FAM (Fluorescein amidite; Molecular Probes, Eugene, OR) and the 3 quencher was TAMRA (tetramethylrhodamine). The cards also contain the passive reference dye, ROX. There was a log linear increase in fluorescence detected as the concentration of amplified double-stranded product cDNA increased during the reaction. The fluorescence was detected as cycle threshold (Ct) with an ABI 7900 thermal cycler (Applied Biosystems Inc.) during 40 cycles. A standard curve was generated from the different concentrations of the rhesus pool. The slope of the curve was used to calculate the relative picograms of each transcript. Then, the ratio of each transcript to GAPDH was calculated for each sample.

Laser captured serotonin neurons

RNA was extracted from pools of laser-captured neurons from ovx animals treated with placebo, E and E+P (n=3/group) and cDNA was synthesized as previously described (Bethea and Reddy, 2008, 2009).

Preamplification of laser captured samples followed by Taqman qPCR

Each laser captured sample and an aliquot of the rhesus pool cDNA was preamplified with a master mix containing Platinum Taq polymerase and all primer sets of interest (200μM each; separately provided by ABI). The preamplification PCR reaction was run for 14 cycles. The PCR product from the multiplex reaction on the rhesus standard pool was diluted to generate a standard curve for each of the primer sets. The PCR product from the laser-captured samples was diluted 1/20. Then, the preamplified standards and samples were loaded onto the custom Taqman cards for qPCR in 100 μl of reaction mix. There was a log linear increase in fluorescence detected as the concentration of amplified double-stranded product cDNA increased during the reaction. The fluorescence was detected as cycle threshold (Ct) with an ABI 7900 thermal cycler (Applied Biosystems Inc.) during 40 cycles. The slope of the curve was used to calculate the relative picograms of each transcript in the RNA extracted from the laser-captured pools. Then, the ratio of each transcript to GAPDH was calculated for each sample.

Validation of Primers

Initially, each primer set (provided separately by ABI) was tested individually with cDNA from the pool of rhesus tissues and from a microdissected dorsal raphe block. The amplification was examined with the ABI 7900 thermal cycler (Applied Biosystems Inc.) during 40 cycles. Each primer set produced a single amplicon as expected.

Hormone Assays

Assays for estrogen and progesterone were performed utilizing a Roche Diagnostics 2010 Elecsys assay instrument. Prior to these analyses, measurements of estradiol and progesterone on this platform were compared to traditional RIA s as previously reported (Bethea et al., 2005).

Statistics

Differences in the percent positive fiber area (pixels), the percent of positive receptor area (pixels), the number of immunopositive cells and the relative mRNA between the groups were determined with a parametric ANOVA followed by Student-Neuman-Keuls posthoc pairwise comparison using Prism Statistical software v5.0 (Graph-Pad Software, Inc., San Diego, CA, USA) and $p < 0.05$ was considered statistically significant.

Results

The effect of ovarian steroid treatment for one month on the transcripts for the urocortins, the CRF receptors and CRFBP was first examined in hemi-midbrain blocks obtained as shown in Figure 1, **panel A** (n=4 animals/group; gift of Dr. Henryk Urbanski). Ovarian steroid treatment did not change the expression of GAPDH in the hemi-midbrain blocks of tissue. Therefore, GAPDH was used to normalize expression of the individual transcripts and the results were expressed a ratio. TPH2 was increased by E and E+P treatment as previously reported (Sanchez et al., 2005). The ratio of TPH2/GAPDH in the Ovx, E and E +P treated groups equaled 1.8±0.6, 277.6±74.2 and 166.9±15.53, respectively (ANOVA $p < 0.0051$), indicating that steroid treatment was effective.

Ovarian steroid treatment significantly changed the expression of CRF-R1 and CRF-R2 in the hemi-midbrain block and the ratio of each transcript to GAPDH is illustrated in Figure 2, **panels A and B.** E- and E+P administration caused a significant decrease in the expression of CRF-R1. In contrast, E and E+P treatment caused a significant increase in CRF-R2 expression although addition of P decreased CRF-R2 expression from that observed with E alone.

The relative expression of UCN1, UCN2 and UCN3 was also changed in the hemi -midbrain block with E or E+P treatment and the results are shown in Figure 2, **panels C, D and E.** UCN1 mRNA was significantly increased by E treatment and suppressed by supplemental P treatment. UCN2 and UCN3 mRNAs were on the order of 100 to 1000-fold lower than UCN1. There was no regulation of UCN2, but UCN3 was significantly decreased by E and E+P treatment. However, UCN3 was at the limit of detection of the assay so these results should be received with caution.

The relative expression of CRFBP was significantly increased with E treatment and suppressed by supplemental P treatment (Figure 2, **panel F**). CRFBP mRNA was reported in the raphe and trigeminal nuclei, which are present in our hemi-midbrain block (Potter et al., 1992).

Because the block of tissue contains many different cell types, it was important to address the question of whether CRF-R1 and CRF-R2 are expressed by serotonin neurons. We utilized laser captured serotonin neurons from ovariectomized monkeys treated with placebo, E or E+P for one month (n=3/group). As illustrated in Figure 1, **panel B,** the serotonin neurons were captured from 7 μm coronal sections through the dorsal raphe of the pontine midbrain. In a previous study, Rhesus Affymetrix microarrays were probed with labeled RNA from the laser captured serotonin neurons and the results were analyzed with GeneSifter. [Subsets of the results have been previously published (Bethea and Reddy, 2008,2009)]. The results were reviewed for expression of CRF-R1 and CRF-R2. The microarray signal intensity for CRF-R1 equaled 160.2±117, 38.5±24 and 33.6±113 for placebo, E and E+P treated animals, respectively (n=2/group). The microarray signal intensity for CRF-R2 equaled 75.1±44, 46.3±3 and 140±116 for placebo, E and E+P treated animals, respectively (n=2 animals/group). These values were not above the threshold for present call on the microarray due to the low copy number. Nonetheless, the trends warranted further examination with qRT-PCR, including a preamplification step. Therefore, samples of the rhesus pool and laser captured serotonin neurons from placebo, E and E+P treated animals (n=3/group) were preamplified and then subjected to qPCR on the custom Taqman cards. As illustrated in Figure 3, E and E+P treatments significantly decreased CRF-R1 expression and significantly increased CRF-R2 expression in laser captured serotonin neurons indicating that serotonin neurons express the CRF receptors in a regulated manner.

CRF neurons in the PVN and amygdala project to the dorsal and median raphe nuclei (Luiten et al., 1985, Portillo et al., 1998). Thus, the mRNA for CRF is largely located elsewhere although small populations of CRF neurons have been detected in the midbrain (Austin et al., 1995). To determine if ovarian steroids regulate the amount of CRF reaching the dorsal and median raphe, CRF fibers were immunostained and quantified in these regions of ovariectomized macaques treated with placebo, E or E+P (n=5 animals/group). CRF fibers were examined in the dorsal and median raphe of 25 μm coronal sections through the pontine midbrain as illustrated in Figure 1, **panel B.** CRF fiber staining was robust in the dorsal and median raphe as illustrated in Figure 4. Three areas were further analyzed as illustrated. The areas were designated dorsal raphe, interfascicular raphe and median raphe. In all areas, it appeared that there was a reduction in fiber density in E- and E +P-treated animals compared to the placebo treated animals. The fiber staining was segmented and expressed as positive pixels. The pixel analyses of the dorsal, interfascicular and median raphe nuclei are shown in Figure 5. Four levels of the midbrain raphe nuclei at 500 μm intervals were examined and the CRF positive pixels were expressed as a percent of the total area. E and E+P treatments caused a significant decrease in the average percent CRF positive pixels at each of the 4 levels in all areas (data not shown). When the average percent CRF positive pixel area was obtained for each group (average of all 4 levels/animal

and then average of 5 animals/group), there was a significant decrease in the overall average percent CRF positive pixel area, or CRF fiber density, in the dorsal, interfascicular and median raphe nuclei with E or E+P administration for one month as illustrated in Figure 5.

To determine if CRF receptor protein expression reflected gene expression, immunocytochemistry for CRF type 1 and type 2 receptors was conducted. CRF-R1 immunostaining is illustrated in Figure 6. **Panel A** illustrates staining in the dorsal raphe at the concentration of primary antibody used for the experimental sections (1/500). **Panel B** illustrates staining in the dorsal raphe at the lowest concentration of primary antibody that produced any detectable signal (1/2000). Preabsorption of the antibody at 1/2000 with the peptide that was used to produce the antibody (500μg) prevented specific staining as illustrated in **Panel C.** In the experimental sections, the receptor staining was segmented and expressed as positive pixels. Five levels of the dorsal raphe at 500 μm intervals were examined in ovariectomized macaques treated with placebo, E or E+P (n=3 animals/group) and the CRF-R1 positive pixels were expressed as a percent of the total area. The pixel analysis of the dorsal raphe nucleus is shown in Figure 7. E and E+P treatments caused a decrease in the average percent CRF-R1 positive pixels at each of the 5 levels with level 3 reaching statistical significance (data not shown). When the average percent CRF-R1 positive pixel area was obtained for each group (average of all 5 levels/animal and then average of 3 animals/group), there was a significant decrease in the overall average percent CRF-R1 positive pixel area in the dorsal raphe nucleus with E and E+P treatment (Figure 7). This is reflective of the gene expression observed in the hemi-midbrain block and in the laser captured serotonin neurons.

CRF-R2 immunostaining at the boundary of the interfascicular raphe and median raphe is illustrated in Figure 8. **Panels A and B** illustrate the immunostaining at the concentration of primary antibody used for the experimental sections (1/750) at a low and high magnification. Panel C illustrates the staining when the antibody at a concentration of 1/750 was preabsorbed with the peptide (1 mg) that was used to produce the antibody. No specific immunostaining was observed after preabsorption of the antibody. In the experimental sections, the receptor staining was segmented and expressed as positive pixels. Five levels of the dorsal and median raphe nuclei at 500 μm intervals were examined in ovariectomized macaques treated with placebo, E or E+P (n=5 animals/group) and the CRF-R2 positive pixels were expressed as a percent of the total area. The pixel analysis of the dorsal and median raphe nuclei is shown in Figure 9. E treatment caused a significant increase in the average percent of CRF-R2 positive pixel area at each of the 5 levels of the dorsal and median raphe (data not shown). In addition, when the average percent of CRF-R2 positive pixel area was obtained for each group (average of all 5 levels/animal and then average of 5 animals/group), there was a significant increase in the overall CRF-R2 positive pixel area in the dorsal and median raphe nuclei with E treatment. However, the stimulatory effect of E was blocked with supplemental P administration. This is reflective of the observed gene expression in the hemi-midbrain block and in the laser captured serotonin neurons.

Examination of gene expression for the urocortins indicated that UCN1 was the predominant transcript in the midbrain and that it was increased by E treatment, and supplemental P treatment blocked the effect of E. The expression of UCN2 and 3 was too low to warrant pursuit at the protein level. The cells that produce UCN1 are located in the rostral midbrain in the supraoculomotor (SOA) area bordering the Edinger-Westfal nucleus (May et al., 2008). To examine the expression of UCN1 at the protein level, the cell bodies and a fiber tract located caudal to the cell bodies (approximately at the level of the caudal linear nucleus) were immunostained and analyzed. Figure 10, **top row** illustrates UCN1 neurons in 4 out of the 8 levels (rostral to caudal) of the midbrain that were examined. A complete map of the midbrain UCN1 neurons in macaque is published in May et al (May et al., 2008). In

addition, the appearance of UCN1 neurons in representative sections from placebo, E and E +P treated monkeys is illustrated in the **bottom row,** Figure 10. A montage of each level was built and the positive cells were marked and tallied with Slidebook 4.2. The total number of UCN1 positive cells in 8 levels of the SOA in each treatment group (n= 5 animals/group) is illustrated in Figure 11, **top panel**. One month of E or E+P treatment caused a significant increase in the number of detectable UCN1 positive neurons at nearly every level (data not shown) and a significant increase in the overall average number of UCN1 positive neurons. In addition, the immunostained area was segmented and the positive pixels were calculated as a percent of the total area examined. E or E+P significantly increased the number of UCN1-positive neurons in 7 of 8 levels analyzed and when the levels were combined (average of all 8 levels/animal and then average of 5 animals/group), there was a significant increase in the percent of UNC1 positive-pixels as illustrated in Figure 11, **bottom panel.**

The UCN1 fiber tract in the area of the caudal linear nucleus is illustrated in Figure 12, which contains representative sections from placebo, E and E+P treated monkeys. The positive fibers have been segmented from the background in blue for clarity. The UCN1 fibers were examined in 3 levels of the midbrain at 500 μm intervals. There appears to be an increase in UCN1 fiber density with E and E+P treatments. For quantification, the pixel area of the positive fibers was obtained and expressed a percent of the total area examined. The results are illustrated in Figure 13. There was a significant increase in UCN1 fiber density (positive pixel area/total area) with E and E+P treatment at all 3 levels (data not shown) and a significant increase in the overall average UCN1 fiber density (average of all 3 levels/ animal and then average of 5 animals/group; Figure 13).

To determine if the effect of estrogen on UCN1 expression may be direct or indirect, UCN1 neurons were immunostained for ERα or ERβ. ERα was not detected. However, nuclear staining for ERβ was evident in UCN1 neurons as well as, other neurons in the area (Figure 14).

Serum estrogen concentrations (pg/ml±sem) in Ovx, E-treated, and E+P treated animals, respectively equaled 8.4±1.7, 78.6±7.1, and 89.0±12.7 in the animals used for immunocytochemistry, 9.6±4.0, 117.0±6.7 and 130±9.5 in the animals for hemi-midbrain block qRT-PCR, and <20, 153±10.9, and 187±3.2 in the animals used for laser capture of serotonin neurons. Serum progesterone concentrations (ng/ml±sem) in Ovx, E-treated, and E +P treated animals, respectively equaled 0.09±0.02, 0.14±0.02, and 3.8±0.7 in the animals used for immunocytochemistry, <0.2, <0.2 and 3.8±0.4 in the animals for hemi-midbrain block qRT-PCR, and 0.23±0.003, 0.24±0.03 and 7.08±1.17 in the animals used for laser capture of serotonin neurons.

Discussion

During and after menopause a significant number of women report an increase in anxiety and vulnerability to stress (Maki et al., Conde et al., 2006, Heikkinen et al., 2006, Tangen and Mykletun, 2008). Both the CRF and serotonin systems respond to stress and play roles in depression and anxiety disorders (Mann et al., 1996, Holsboer, 1999, Keck and Holsboer, 2001, Arango et al., 2002). Moreover, increasing evidence suggests that their function is inextricably linked. In humans, CRF terminals appose serotonin neurons in the raphe region (Ruggiero et al., 1999), and a postmortem study reported that patients with major depressive disorder had significantly more CRH-positive neurons in the PVN than normal controls (Raadsheer et al., 1994). Antidepressant SSRIs that increase available serotonin reduce the sensitivity of CRF neurons in the PVN (Stout et al., 2002b), and cortisol levels return to normal in depressed patients treated with a variety of antidepressants (Himmerich et al.,

2006, Schule et al., 2006). Moreover, repeated treatment with citalopram, an SSRI, decreased CRF and HPA axis activity in rodents (Moncek et al., 2003). We recently found that 15 weeks of citalopram administration decreased CRF fiber density in the dorsal raphe of stress-sensitive monkeys (Weissheimer et al., 2009).

The impact of ovarian steroids on mental function is of significant importance to women as they transition through menopause. Women without a uterus may be prescribed a formulation of estrogen, whereas women with a uterus may be prescribed a formulation of estrogen supplemented with progestin to prevent uterine hypertrophy. Therefore, we applied a paradigm in which ovariectomized monkeys are used as a model of surgical menopause and groups treated with placebo, estradiol alone or estradiol supplemented with progesterone were compared.

In the absence of hormone therapy, postmenopausal women exhibit higher release of ACTH and cortisol when administered a challenge of dexamethasone plus CRH (Kudielka et al., 1999) suggesting that their CRF system may be hyperactive. In animal models, the effects of ovarian steroids on the HPA axis are complex. Several studies initially indicated that treatment of ovariectomized female or male rats with estrogen increased CRF (Li et al., 2003, Lund et al., 2004). Subsequently, it was recognized that acute E treatment increases CRF, but low dose chronic E treatment decreased CRH in a stressed rodent model (Dayas et al., 2000). Likewise, 5 days of E treatment to ovariectomized macaques prevented the elevation in cortisol induced by icv administration of interleukin 1-alpha (Xia-Zhang et al., 1995), and we found that chronic hormone replacement in ovariectomized monkeys decreased CRF mRNA and protein in the PVN (Bethea and Centeno, 2008).

However, CRF expression is widespread in the brain and within the limbic system there is evidence that the CRH system modulates behavioral traits such as locomotor activity, sleep, addictive behavior and in particular, anxiety related behavior (Dunn and Berridge, 1990, Liebsch et al., 1995). Indeed, we found that in stress-sensitive macaques, CRF mRNA was elevated in the subthalamic nucleus as well as the PVN, and that CRF fiber density was greater in the central nucleus of the amgydala compared to stress-resilient macaques (Centeno et al., 2007).

The knowledge of CRF innervation of the serotonergic raphe nuclei (Sakanaka et al., 1987, Ruggiero et al., 1999) coupled with the detection of CRF receptors in the raphe (Chalmers et al., 1995, Van Pett et al., 2000) forged the link between the CRF and serotonin systems. Subsequently, the opposing effects of CRF and UCN on serotonin were established in rodents. Administration of CRF directly into the DRN inhibits serotonergic activity, and CRF-R1 antagonists block this effect (Denihan et al., 2000). Conversely, the stimulatory effect of UCN and CRF-R2 is supported by increased 5-HT efflux in the basolateral amygdala (a projection region of the DRN) with intra-DRN administration of the CRF-R2 agonist, UCN2. This effect was completely blocked by antisauvagine-30 (ASV-30), a relatively selective CRF-R2 antagonist (Amat et al., 2004).

This study in monkeys shows that E±P decreased CRF fiber density in the dorsal, interfasicular and median raphe suggesting that CRF transport to the serotonin system is lower in the presence of ovarian steroids. The origin of the CRF fibers in the raphe nuclei is likely the PVN, but it is premature to rule out other areas of origin given the expression of CRF in amygdala and subthalamic nuclei. Previous work also traced CRF terminals in the raphe to cell bodies in the dorsolaterial tegmental field (Sakai et al., 1977). These data raise the question of whether the CRF cell bodies contain any form of estrogen receptors, and/or whether CRF neurons may differ in their expression of receptors from region to region? In rodents, Laflamme et al (Laflamme et al., 1998) reported that non-neuroendocrine CRF

neurons in the caudal PVN expressed ERβ [these neurons project to the raphe (Luiten et al., 1985, Portillo et al., 1998)]. However, few neuroendocrine CRF neurons in the medial PVN expressed ERβ [project to the median eminence and regulate ACTH]. Another study reported ERα in CRF neurons in human hypothalamus (Bao et al., 2005). The CRF gene lacks a classical ERE site and *in vitro* studies suggest that ERβ stimulates CRF transcription in HeLa cells through alternate pathways (Miller et al., 2004, Ni and Nicholson, 2006). The latter data cannot be reconciled with our observations that estrogen decreases CRF in primates (Bethea and Centeno, 2008). We speculate that E±P increases serotonin, which in turn, decreases CRF in the PVN via inhibitory interneurons and this is reflected by a decrease in fiber density in the raphe.

We found that E±P decreased CRF-R1 at the gene and protein levels in the raphe nuclei suggesting that ovarian steroids downregulate expression of the angiogenic receptor. In contrast, E increased CRF-R2 in the dorsal raphe nucleus suggesting that estrogens increase expression of the angiolytic receptor. We have shown that serotonin neurons express ERβ and PR (Bethea, 1993, Gundlah et al., 2001), which could regulate CRF-R1 or R2 expression. However, our immunocytochemical studies do not reveal whether the receptors are expressed on serotonin neurons. Rather, our qRT-PCR on RNA from laser captured serotonin neurons indicated that CRF-R1 was downregulated and CRF-R2 was upregulated, indicating that serotonin neurons express both receptors. However, the laser capture material is not pure, rather it is enriched about 7–10 fold for serotonin neuron RNA, so we cannot completely rule out the possibility that the receptor RNA was contributed by other neurons. CRF-R1 was not detectable by autoradiography or ISH in the raphe of rats (Day et al., 2004) or monkeys (Sanchez et al., 1999), but CRF-R1 immunostaining was demonstrated in the raphe of monkeys with a well-characterized and highly specific antibody (Kostich et al., 2004). In our study, CRF-R1 immunostaining was clearly present, but we also detected CRF-R1 mRNA suggesting that the Taqman qPCR may be more sensitive than the other approaches. In rodents, double ISH revealed that CRF-R2 was expressed exclusively in serotonin neurons at midlevels of the dorsal raphe, whereas, at caudal levels, CRF-R2 was expressed in both serotonin and GABAergic neurons (Day et al., 2004). In addition, administration of UCN2 into the DRN increased c-fos expression in labeled 5-HT neurons (Amat et al., 2004).

E alone increased UCN1 expression and P blocked this action at the gene level, but at the protein level there was an increase in immunostained neurons in the SOA and an increase in fiber density rostral to the raphe nuclei with E alone and E+P. We cannot explain the disconnection between gene and protein expression with supplemental P, but our data indicate that part of the action of E was through nuclear ERβ. UNC1 colocalizes with CART (Kozicz, 2003) and we previously detected PR in the same population of UCN1/CART neurons (Lima et al., 2008). Hence, UCN1 neurons have nuclear ERβ and PR, indicating they are direct targets of ovarian steroids.

The increase observed in CRFBP with E treatment could be anti-anxiety as well. CRFBP is thought to bind CRF and prevent it from binding to receptors. Since CRF has the highest affinity at CRF-R1, any decrease in CRF due to CRFBP binding would first prevent its activation of the preferred angiogenic CRF-R1 receptors. CRFBP mRNA and immunostaining were reported in the trigeminal nuclei and in some raphe nuclei of pontine midbrain (Potter et al., 1992), which are present in our hemi-midbrain block.

The mechanisms of action of E and P on the different components under study may differ from gene to gene. Classically E acts through nuclear ERs that bind to E response elements (EREs) and stimulate gene transcription. The stimulatory effect of E was observed in the expression of CRF-R2 and UCN1 at gene levels, which was translated to the protein level. P

was observed to block the effect of E on CRF-R2 gene and protein expression, and to block the effect of E on UCN1 and CRFBP gene expression. However, P did not block the effect of E on UCN1 protein expression. In the presence of E, supplemental P administration can have different effects depending on the gene, the ratio of E/P achieved in the serum and the isoforms of progestin receptor (PR) in the cell type. At the ratio of 1/50 typically achieved with our implants, P has been observed to block E -stimulated PR gene expression in the pituitary, but to have no effect on E-stimulated PR gene expression in the hypothalamus of the same animals (Bethea et al., 1996). This may be due to the differential prevalence of PR-A and PR-B in pituitary and brain (Bethea and Widmann, 1998). P is also converted to allopregnanolone, which binds to the GABA receptor and exhibits sedative properties similar to benzodiazapenes (Barbaccia et al., 2001). Perhaps P decreased UCN1 gene expression via nuclear PR action, but allopregnanolone promoted RNA stability and protein expression. Studies to better distinguish the actions of P through nuclear PR, membrane PR and converson to allopreganolone are greatly needed.

In contrast, E±P decreased gene and protein expression of CRF-R1. The ability of E to decrease gene expression appears to rely on indirect mechanisms. In one pathway, ligand activated steroid receptors sequester NFkB and thereby decrease gene transcription that is dependent upon binding of NFkB to its response element, NRE (Cerillo et al., 1998, McKay and Cidlowski, 1999). Hence, genes that are driven by NFkB can be deactivated with E treatment. There is precidence to speculate that stress signals induce translocation of NFkB to the nucleus where it drives CRF-R1 gene expression, and that E decreases this action by incapacitating NFkB. Indeed, we have shown that E treatment decreases NFkB translocation to the nucleus in serotonin neurons of the dorsal raphe (Bethea et al., 2006).

Altogether, in addition to direct actions of E and P on serotonin related gene expression, these data support the notion that ovarian steroids increase serotonin neural function by actions through the CRF system, which include decreased CRF transported to serotonin neurons and a decrease in CRF-R1 expression, in conjunction with an increase in UCN1 transported caudally and an increase in CRF-R2 and CRFBP expression. An increase in serotonin function would elevate mood, increase stress resilience and decrease anxiety (Graeff, 2002, Hammack et al., 2002, Hanley and Van de Kar, 2003, Hendricks et al., 2003, Lowry et al., 2009). From the opposite perspective, stress increases CRF production, which under chronic conditions could decrease serotonin neurotransmission resulting in depression and anxiety (Stout et al., 2002a, Valentino et al., 2009). Our data indicate that ovarian steroids may be protective by ameliorating (not necessarily blocking) these effects of stress, and that the absence of ovarian steroids, as in menopause, would increase sensitivity to stress.

In our cynomolgus model of sensitivity to stress-induced reproductive dysfunction, the stress-sensitive animals exhibit elevated CRF in the PVN (Centeno et al., 2007) and higher CRF fiber density in the dorsal raphe nucleus (Weissheimer, 2010) *in the absence of external stress.* Moreover, administration of the selective serotonin reuptake inhibitor, s-citalopram, reduced CRF fiber density in the dorsal raphe of the stress-sensitive monkeys (Weissheimer, 2010). There are numerous studies in humans indicating that childhood trauma leads to vulnerability to stress and affective disorders in adulthood (Nemeroff, 2004a), Since the cynomolgus monkeys are caught and imported, we speculate that the vulnerability of some individuals is due to “childhood trauma” in the wild such as variable foraging demands on the mother or abuse (Coplan et al., 2010).

In conclusion, it is well accepted that CRF regulates serotonin and conversely, serotonin regulates CRF. As illustrated in Figure 15, our data strongly indicate that ovarian steroids regulate both systems in primates in a synergistic manner. That is, either E alone or E+P act

through nuclear, and perhaps other, receptors in serotonin neurons to increase serotonin function. At the same time, they act either directly or indirectly to decrease CRF, to decrease CRF-R1, to increase UCN1 and to increase CRF-R2 in the raphe terminal fields. Although ER has been detected in CRF neurons, the CRF gene has ERE half-sites and cellular studies do not agree with the whole animal physiology (Miller et al., 2004). Therefore, we speculate that the steroid induced increase in serotonin acts to decrease CRF in the PVN via interneurons (Bethea and Centeno, 2008). This in turn, results in less CRF delivered back to the serotonin neurons, further removing inhibition and increasing serotonin delivered to CRF neurons. Perhaps we can cautiously surmise that ovarian steroids start and/or optimally maintain a critical feed-forward loop between the serotonin and CRF neural systems in primates, which is beneficial to mental health and coping strategies.

Acknowledgments

This work was supported by NIH grants: MH62677 to CLB, T32-DK07680 (Multidisciplinary Training in Neuroendocrinology, PI Richard Goodman) and T32-HD007133 (Training in Reproductive Biology, PI Sergio Ojeda) to RLS, U54 contraceptive Center Grant HD 18185 (PI Richard Stouffer)and RR00163 for the operation of ONPRC.

Rachel L. Sanchez conducted the majority of this work as part of the requirements for a Ph.D. from Oregon Health and Science University. Portions of this study were presented at the 2008 Annual Meeting of the Endocrine Society, and the 2008 and 2009 Annual Meetings of the Society for Neuroscience. We greatly appreciate the time and effort devoted by Dr. Jessica Henderson to preparation of the animals and sectioning of the tissue for ICC. We thank Dr. Wylie Vale for his generous gift of antiserum to human CRH. We thank Dr. Henryk Urbanski for the hemi-midbrain tissue blocks used for qRT-PCR. We are indebted to the dedicated technicians of the Division of Animal Resources for their outstanding care and attention to the health and well being of our monkeys.

Literature Cited

Amat J, Tamblyn JP, Paul ED, Bland ST, Amat P, Foster AC, Watkins LR, Maier SF. Microinjection of urocortin 2 into the dorsal raphe nucleus activates serotonergic neurons and increases extracellular serotonin in the basolateral amygdala. Neuroscience. 2004; 129:509–519. [PubMed: 15541873]

Arango V, Underwood MD, Mann JJ. Serotonin brain circuits involved in major depression and suicide. Prog Brain Res. 2002; 136:443–453. [PubMed: 12143401]

Austin MC, Rice PM, Mann JJ, Arango V. Localization of corticotropin-releasing hormone in the human locus coeruleus and pedunculopontine tegmental nucleus: an immunocytochemical and in situ hybridization study. Neuroscience. 1995; 64:713–727. [PubMed: 7715783]

Bao AM, Hestiantoro A, Van Someren EJ, Swaab DF, Zhou JN. Colocalization of corticotropin-releasing hormone and oestrogen receptor-alpha in the paraventricular nucleus of the hypothalamus in mood disorders. Brain. 2005; 128:1301–1313. [PubMed: 15705605]

Barbaccia ML, Serra M, Purdy RH, Biggio G. Stress and neuroactive steroids. Int Rev Neurobiol. 2001; 46:243–272. [PubMed: 11599302]

Bassett JL, Foote SL. Distribution of corticotropin-releasing factor-like immunoreactivity in squirrel monkey (Saimiri sciureus) amygdala. J Comp Neurol. 1992; 323:91–102. [PubMed: 1430317]

Behan DP, De Souza EB, Lowry PJ, Potter E, Sawchenko P, Vale WW. Corticotropin releasing factor (CRF) binding protein: a novel regulator of CRF and related peptides. Front Neuroendocrinol. 1995a; 16:362–382. [PubMed: 8557170]

Behan DP, Maciejewski D, Chalmers D, De Souza EB. Corticotropin releasing factor binding protein (CRF-BP) is expressed in neuronal and astrocytic cells. Brain Res. 1995b; 698:259–264. [PubMed: 8581494]

Bethea CL. Colocalization of progestin receptors with serotonin in raphe neurons of macaque. Neuroendocrinology. 1993; 57:1–6. [PubMed: 8479605]

Bethea CL. Regulation of progestin receptors in raphe neurons of steroid-treated monkeys. Neuroendocrinology. 1994; 60:50–61. [PubMed: 8090282]

Bethea CL, Brown NA, Kohama SG. Steroid regulation of estrogen and progestin receptor messenger ribonucleic acid in monkey hypothalamus and pituitary. Endocrinology. 1996; 137:4372–4383. [PubMed: 8828498]

Bethea CL, Centeno ML. Ovarian steroid treatment decreases corticotropin-releasing hormone (CRH) mRNA and protein in the hypothalamic paraventricular nucleus of ovariectomized monkeys. Neuropsychopharmacology. 2008; 33:546–556. [PubMed: 17507918]

Bethea CL, Lu NZ, Gundlah C, Streicher JM. Diverse actions of ovarian steroids in the serotonin neural system. Front Neuroendocrinol. 2002; 23:41–100. [PubMed: 11906203]

Bethea CL, Reddy AP. Effect of ovarian hormones on survival genes in laser captured serotonin neurons from macaques. J Neurochem. 2008; 105:1129–1143. [PubMed: 18182058]

Bethea CL, Reddy AP. Effect of ovarian hormones on genes promoting dendritic spines in laser-captured serotonin neurons from macaques. Mol Psychiatry. 2009 E pub ahead of print.

Bethea CL, Reddy AP, Smith LJ. Nuclear factor kappa B in the dorsal raphe of macaques: an anatomical link for steroids, cytokines and serotonin. J Psychiatry Neurosci. 2006; 31:105–114. [PubMed: 16575426]

Bethea CL, Reddy AP, Tokuyama Y, Henderson JA, Lima FB. Protective actions of ovarian hormones in the serotonin system of macaques. Front Neuroendocrinol. 2009; 30:212–238. [PubMed: 19394356]

Bethea CL, Streicher JM, Mirkes SJ, Sanchez RL, Reddy AP, Cameron JL. Serotonin-related gene expression in female monkeys with individual sensitivity to stress. Neuroscience. 2005; 132:151–166. [PubMed: 15780474]

Bethea CL, Widmann AA. Differential espression of progestin receptor isoforms in the hypothalamus, pituitary, and endometrium or rhesus macaques. Endocrinology. 1998; 139:677–687. [PubMed: 9449641]

Centeno ML, Sanchez RL, Reddy AP, Cameron JL, Bethea CL. Corticotropin-releasing hormone and pro-opiomelanocortin gene expression in female monkeys with differences in sensitivity to stress. Neuroendocrinology. 2007; 86:277–288. [PubMed: 17934253]

Cerillo G, Rees A, Manchanda N, Reilly C, Brogan I, White A, Needham M. The oestrogen receptor regulates NFkappaB and AP-1 activity in a cell-specific manner. Journal of Steroid Biochemical Molecular Biology. 1998; 67:79–88.

Chalmers DT, Lovenberg TW, De Souza EB. Localization of novel corticotropin-releasing factor receptor (CRF2) mRNA expression to specific subcortical nuclei in rat brain: comparison with CRF1 receptor mRNA expression. J Neurosci. 1995; 15:6340–6350. [PubMed: 7472399]

Conde DM, Pinto-Neto AM, Santos-Sa D, Costa-Paiva L, Martinez EZ. Factors associated with quality of life in a cohort of postmenopausal women. Gynecol Endocrinol. 2006; 22:441–446. [PubMed: 17012106]

Coplan JD, Abdallah CG, Kaufman J, Gelernter J, Smith EL, Perera TD, Dwork AJ, Kaffman A, Gorman JM, Rosenblum LA, Owens MJ, Nemeroff CB. Early-life stress, corticotropin-releasing factor, and serotonin transporter gene: A pilot study. Psychoneuroendocrinology. 2010

Dautzenberg FM, Hauger RL. The CRF peptide family and their receptors: yet more partners discovered. Trends Pharmacol Sci. 2002; 23:71–77. [PubMed: 11830263]

Day HE, Greenwood BN, Hammack SE, Watkins LR, Fleshner M, Maier SF, Campeau S. Differential expression of 5HT-1A, alpha 1b adrenergic, CRF-R1, and CRF-R2 receptor mRNA in serotonergic, gamma-aminobutyric acidergic, and catecholaminergic cells of the rat dorsal raphe nucleus. J Comp Neurol. 2004; 474:364–378. [PubMed: 15174080]

Dayas CV, Xu Y, Buller KM, Day TA. Effects of chronic oestrogen replacement on stress-induced activation of hypothalamic-pituitary-adrenal axis control pathways. J Neuroendocrinol. 2000; 12:784–794. [PubMed: 10929091]

de Kloet ER, Joels M, Holsboer F. Stress and the brain: from adaptation to disease. Nat Rev Neurosci. 2005; 6:463–475. [PubMed: 15891777]

Denihan A, Kirby M, Bruce I, Cunningham C, Coakley D, Lawlor BA. Three-year prognosis of depression in the community-dwelling elderly. British Journal of Psychiatry. 2000; 176:453–457. [PubMed: 10912221]

Dunn AJ, Berridge CW. Physiological and behavioral responses to corticotropin-releasing factor administration: is CRF a mediator of anxiety or stress responses? Brain Res Brain Res Rev. 1990; 15:71–100. [PubMed: 1980834]

Graeff FG. On serotonin and experimental anxiety. Psychopharmacology (Berl). 2002; 163:467–476. [PubMed: 12373447]

Gundlah C, Lu NZ, Mirkes SJ, Bethea CL. Estrogen receptor beta (ERb) mRNA and protein in serotonin neurons of macaques. Mol Brain Research. 2001; 91:14–22.

Gundlah C, Pecins-Thompson M, Schutzer WE, Bethea CL. Ovarian steroid effects on serotonin 1A, 2A and 2C receptor mRNA in macaque hypothalamus. Mol Brain Research. 1999; 63:325–339.

Hammack SE, Richey KJ, Schmid MJ, LoPresti ML, Watkins LR, Maier SF. The role of corticotropin-releasing hormone in the dorsal raphe nucleus in mediating the behavioral consequences of uncontrollable stress. J Neurosci. 2002; 22:1020–1026. [PubMed: 11826130]

Hanley NR, Van de Kar LD. Serotonin and the neuroendocrine regulation of the hypothalamic--pituitary-adrenal axis in health and disease. Vitam Horm. 2003; 66:189–255. [PubMed: 12852256]

Heikkinen J, Vaheri R, Timonen U. A 10-year follow-up of postmenopausal women on long-term continuous combined hormone replacement therapy: Update of safety and quality-of-life findings. J Br Menopause Soc. 2006; 12:115–125. [PubMed: 16953985]

Hendricks TJ, Fyodorov DV, Wegman LJ, Lelutiu NB, Pehek EA, Yamamoto B, Silver J, Weeber EJ, Sweatt JD, Deneris ES. Pet-1 ETS gene plays a critical role in 5-HT neuron development and is required for normal anxiety-like and aggressive behavior. Neuron. 2003; 37:233–247. [PubMed: 12546819]

Himmerich H, Binder EB, Kunzel HE, Schuld A, Lucae S, Uhr M, Pollmacher T, Holsboer F, Ising M. Successful antidepressant therapy restores the disturbed interplay between TNF-alpha system and HPA axis. Biol Psychiatry. 2006; 60:882–888. [PubMed: 16989778]

Holsboer F. The rationale for corticotropin-releasing hormone receptor (CRH-R) antagonists to treat depression and anxiety. J Psychiatr Res. 1999; 33:181–214. [PubMed: 10367986]

Keck ME, Holsboer F. Hyperactivity of CRH neuronal circuits as a target for therapeutic interventions in affective disorders. Peptides. 2001; 22:835–844. [PubMed: 11337098]

Keck ME, Ohl F, Holsboer F, Muller MB. Listening to mutant mice: a spotlight on the role of CRF/CRF receptor systems in affective disorders. Neurosci Biobehav Rev. 2005; 29:867–889. [PubMed: 15899517]

Kemp CF, Woods RJ, Lowry PJ. The corticotrophin-releasing factor-binding protein: an act of several parts. Peptides. 1998; 19:1119–1128. [PubMed: 9700765]

Kostich WA, Grzanna R, Lu NZ, Largent BL. Immunohistochemical visualization of corticotropin-releasing factor type 1 (CRF1) receptors in monkey brain. J Comp Neurol. 2004; 478:111–125. [PubMed: 15349973]

Kozicz T. Neurons colocalizing urocortin and cocaine and amphetamine-regulated transcript immunoreactivities are induced by acute lipopolysaccharide stress in the Edinger-Westphal nucleus in the rat. Neuroscience. 2003; 116:315–320. [PubMed: 12559087]

Kudielka BM, Schmidt-Reinwald AK, Hellhammer DH, Kirschbaum C. Psychological and endocrine responses to psychosocial stress and dexamethasone/corticotropin-releasing hormone in healthy postmenopausal women and young controls: the impact of age and a two-week estradiol treatment. Neuroendocrinology. 1999; 70:422–430. [PubMed: 10657735]

Laflamme N, Nappi RE, Drolet G, Labrie C, Rivest S. Expression and neuropeptidergic characterization of estrogen receptors (ERalpha and ERbeta) throughout the rat brain: anatomical evidence of distinct roles of each subtype. J Neurobiol. 1998; 36:357–378. [PubMed: 9733072]

Li XF, Mitchell JC, Wood S, Coen CW, Lightman SL, O'Byrne KT. The effect of oestradiol and progesterone on hypoglycaemic stress-induced suppression of pulsatile luteinizing hormone release and on corticotropin-releasing hormone mRNA expression in the rat. J Neuroendocrinol. 2003; 15:468–476. [PubMed: 12694372]

Liebsch G, Landgraf R, Gerstberger R, Probst JC, Wotjak CT, Engelmann M, Holsboer F, Montkowski A. Chronic infusion of a CRH1 receptor antisense oligodeoxynucleotide into the central nucleus of the amygdala reduced anxiety-related behavior in socially defeated rats. Regul Pept. 1995; 59:229–239. [PubMed: 8584759]

Lima FB, Henderson JA, Reddy AP, Tokuyama Y, Hubert GW, Kuhar MJ, Bethea CL. Unique responses of midbrain CART neurons in macaques to ovarian steroids. Brain Res. 2008; 1227:76–88. [PubMed: 18598674]

Lowry CA, Hale MW, Plant A, Windle RJ, Shanks N, Wood SA, Ingram CD, Renner KJ, Lightman SL, Summers CH. Fluoxetine inhibits corticotropin-releasing factor (CRF)-induced behavioural responses in rats. Stress. 2009; 12:225–239. [PubMed: 18951247]

Luiten PG, ter Horst GJ, Karst H, Steffens AB. The course of paraventricular hypothalamic efferents to autonomic structures in medulla and spinal cord. Brain Res. 1985; 329:374–378. [PubMed: 3978460]

Lund TD, Munson DJ, Haldy ME, Handa RJ. Androgen inhibits, while oestrogen enhances, restraint-induced activation of neuropeptide neurones in the paraventricular nucleus of the hypothalamus. J Neuroendocrinol. 2004; 16:272–278. [PubMed: 15049858]

Maki PM, Freeman EW, Greendale GA, Henderson VW, Newhouse PA, Schmidt PJ, Scott NF, Shively CA, Soares CN. Summary of the National Institute on Aging-sponsored conference on depressive symptoms and cognitive complaints in the menopausal transition. Menopause. 17:815–822. [PubMed: 20616668]

Mann JJ, Malone KM, Diehl DJ, Perel J, Cooper TB, Mintun MA. Demonstration in vivo of reduced serotonin responsivity in the brain of untreated depressed patients. Am J Psychiatry. 1996; 153:174–182. [PubMed: 8561196]

May PJ, Reiner AJ, Ryabinin AE. Comparison of the distributions of urocortin-containing and cholinergic neurons in the perioculomotor midbrain of the cat and macaque. J Comp Neurol. 2008; 507:1300–1316. [PubMed: 18186029]

McKay LI, Cidlowski JA. Molecular control of immune/inflammatory responses: interactions between nuclear factor-$_K$B and steroid receptor-signaling pathways. Endocrine Reviews. 1999; 20:435–459. [PubMed: 10453354]

Miller WJ, Suzuki S, Miller LK, Handa R, Uht RM. Estrogen receptor (ER)beta isoforms rather than ERalpha regulate corticotropin-releasing hormone promoter activity through an alternate pathway. J Neurosci. 2004; 24:10628–10635. [PubMed: 15564578]

Moncek F, Duncko R, Jezova D. Repeated citalopram treatment but not stress exposure attenuates hypothalamic-pituitary-adrenocortical axis response to acute citalopram injection. Life Sci. 2003; 72:1353–1365. [PubMed: 12527033]

Morimoto A, Nakamori T, Morimoto K, Tan N, Murakami N. The central role of corticotropin-releasing factor (CRF-41) in psychological stress in rats. J Physiology. 1993; 460:221–229.

Muller MB, Zimmermann S, Sillaber I, Hagemeyer TP, Deussing JM, Timpl P, Kormann MS, Droste SK, Kuhn R, Reul JM, Holsboer F, Wurst W. Limbic corticotropin-releasing hormone receptor 1 mediates anxiety-related behavior and hormonal adaptation to stress. Nat Neurosci. 2003; 6:1100–1107. [PubMed: 12973355]

Nemeroff CB. Neurobiological consequences of childhood trauma. J Clin Psychiatry. 2004a; 65(Suppl 1):18–28. [PubMed: 14728093]

Nemeroff CC. Early-life adversity, CRF dysregulation, and vulnerability to mood and anxiety disorders. Psychopharmacol Bull. 2004b; 38:14–20. [PubMed: 17065965]

Ni X, Nicholson RC. Steroid hormone mediated regulation of corticotropin-releasing hormone gene expression. Front Biosci. 2006; 11:2909–2917. [PubMed: 16720362]

Owens MJ, Nemeroff CB. Role of serotonin in the pathophysiology of depression: focus on the serotonin transporter. Clinical Chemistry. 1994; 40:288–295. [PubMed: 7508830]

Pernar L, Curtis AL, Vale WW, Rivier JE, Valentino RJ. Selective activation of corticotropin-releasing factor-2 receptors on neurochemically identified neurons in the rat dorsal raphe nucleus reveals dual actions. J Neurosci. 2004; 24:1305–1311. [PubMed: 14960601]

Petrov T, Krukoff TL, Jhamandas JH. The hypothalamic paraventricular and lateral parabrachial nuclei receive collaterals from raphe nucleus neurons: a combined double retrograde and immunocytochemical study. J Comp Neurol. 1992; 318:18–26. [PubMed: 1583154]

Portillo F, Carrasco M, Vallo JJ. Separate populations of neurons within the paraventricular hypothalamic nucleus of the rat project to vagal and thoracic autonomic preganglionic levels and

express c-Fos protein induced by lithium chloride. J Chem Neuroanat. 1998; 14:95–102. [PubMed: 9625354]

Potter E, Behan DP, Linton EA, Lowry PJ, Sawchenko PE, Vale WW. The central distribution of a corticotropin-releasing factor (CRF)-binding protein predicts multiple sites and modes of interaction with CRF. Proc Natl Acad Sci U S A. 1992; 89:4192–4196. [PubMed: 1315056]

Raadsheer FC, Hoogendijk WJ, Stam FC, Tilders FJ, Swaab DF. Increased numbers of corticotropin-releasing hormone expressing neurons in the hypothalamic paraventricular nucleus of depressed patients. Neuroendocrinology. 1994; 60:436–444. [PubMed: 7824085]

Ruggiero DA, Underwood MD, Rice PM, Mann JJ, Arango V. Corticotropic-releasing hormone and serotonin interact in the human brainstem: behavioral implications. Neuroscience. 1999; 91:1343–1354. [PubMed: 10391441]

Sakai K, Salvert D, Touret M, Jouvet M. Afferent connections of the nucleus raphe dorsalis in the cat as visualized by the horseradish peroxidase technique. Brain Res. 1977; 137:11–35. [PubMed: 922504]

Sakanaka M, Shibasaki T, Lederis K. Corticotropin releasing factor-like immunoreactivity in the rat brain as revealed by a modified cobalt-glucose oxidase-diaminobenzidine method. J Comp Neurol. 1987; 260:256–298. [PubMed: 3497182]

Sanchez MM, Young LJ, Plotsky PM, Insel TR. Autoradiographic and in situ hybridization localization of corticotropin-releasing factor 1 and 2 receptors in nonhuman primate brain. J Comp Neurol. 1999; 408:365–377. [PubMed: 10340512]

Sanchez RL, Reddy AP, Centeno ML, Henderson JA, Bethea CL. A second tryptophan hydroxylase isoform, TPH-2 mRNA, is increased by ovarian steroids in the raphe region of macaques. Brain Res Mol Brain Res. 2005; 135:194–203. [PubMed: 15857682]

Schule C, Baghai TC, Eser D, Zwanzger P, Jordan M, Buechs R, Rupprecht R. Time course of hypothalamic-pituitary-adrenocortical axis activity during treatment with reboxetine and mirtazapine in depressed patients. Psychopharmacology. 2006; 186:601–611. [PubMed: 16758243]

Smith GW, Aubry JM, Dellu F, Contarino A, Bilezikjian LM, Gold LH, Chen R, Marchuk Y, Hauser C, Bentley CA, Sawchenko PE, Koob GF, Vale W, Lee KF. Corticotropin releasing factor receptor 1-deficient mice display decreased anxiety, impaired stress response, and aberrant neuroendocrine development. Neuron. 1998; 20:1093–1102. [PubMed: 9655498]

Stout SC, Owens MJ, Nemeroff CB. Regulation of corticotropin-releasing factor neuronal systems and hypothalamic-pituitary-adrenal axis activity by stress and chronic antidepressant treatment. J Pharmacol Exp Ther. 2002a; 300:1085–1092. [PubMed: 11861819]

Stout SC, Owens MJ, Nemeroff CB. Regulation of corticotropin-releasing factor neuronal systems and hypothalamic-pituitary-adrenal axis activity by stress and chronic antidepressant treatment. J Pharmacol Exp Ther. 2002b; 300:1085–1092. [PubMed: 11861819]

Tangen T, Mykletun A. Depression and anxiety through the climacteric period: an epidemiological study (HUNT-II). J Psychosom Obstet Gynaecol. 2008; 29:125–131. [PubMed: 18484441]

Timpl P, Spanagel R, Sillaber I, Kresse A, Reul JM, Stalla GK, Blanquet V, Steckler T, Holsboer F, Wurst W. Impaired stress response and reduced anxiety in mice lacking a functional corticotropin-releasing hormone receptor 1. Nat Genet. 1998; 19:162–166. [PubMed: 9620773]

Valdez GR, Inoue K, Koob GF, Rivier J, Vale W, Zorrilla EP. Human urocortin II: mild locomotor suppressive and delayed anxiolytic-like effects of a novel corticotropin-releasing factor related peptide. Brain Res. 2002; 943:142–150. [PubMed: 12088848]

Valentino RJ, Lucki I, Van Bockstaele E. Corticotropin-releasing factor in the dorsal raphe nucleus: Linking stress coping and addiction. Brain Res. 2009

Van Pett K, Viau V, Bittencourt JC, Chan RK, Li HY, Arias C, Prins GS, Perrin M, Vale W, Sawchenko PE. Distribution of mRNAs encoding CRF receptors in brain and pituitary of rat and mouse. J Comp Neurol. 2000; 428:191–212. [PubMed: 11064361]

Vaughan J, Donaldson C, Bittencourt J, Perrin MH, Lewis K, Sutton S, Chan R, Turnbull AV, Lovejoy D, Rivier C, et al. Urocortin, a mammalian neuropeptide related to fish urotensin I and to corticotropin-releasing factor. Nature. 1995; 378:287–292. [PubMed: 7477349]

Weiss JM, Stout JC, Aaron MF, Quan N, Owens MJ, Butler PD, Nemeroff CB. Depression and anxiety: role of the locus coeruleus and corticotropin releasing factor. Brain Research Bulletin. 1994; 35:561–572. [PubMed: 7859114]

Weissheimer, KV.; Herod, SM.; Cameron, JL.; Bethea, CL. The role of stress sensitivity and the effect of citalopram treatment on corticotropin releasing hormone (CRH) and urocortin I (UCN) fiber density in the midbrain raphe region of macaques. Society for Neuroscience; Chicago IL: 2009.

Weissheimer KV, Herod SM, Cameron JL, Bethea CL. Interactions of corticotropin-releasing factor, urocortin and citalopram in a primate model of stress-induced amenorrhea. Neuroendocrinology. 2010 in press.

Xia-Zhang L, Xiao E, Ferin M. A 5-day estradiol therapy, in amounts reproducing concentrations of the early-mid follicular phase, prevents the activation of the hypothalamo-pituitary-adrenal axis by interleukin-1 alpha in the ovariectomized rhesus monkey. J Neuroendocrinol. 1995; 7:387–392. [PubMed: 7550285]

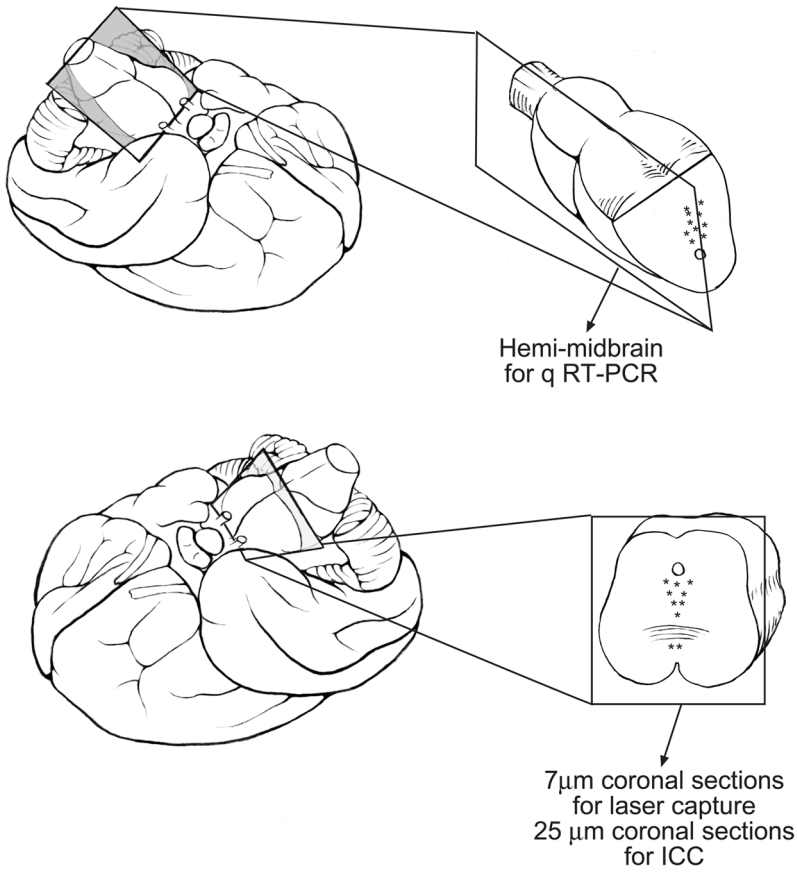

Figure 1.

An Illustration of the dissection of the midbrain and preparation of tissue for assay. **In panel A**, the midbrain and brainstem were removed from the cerebellum and bissected along the saggital plane. One half was immersion fixed in RNA later and then frozen at −80C until RNA extraction for qRT-PCR employing a Taqman Custom Expression Array. **In panel B**, the midbrain was removed from the hypothalamus with a rostral coronal cut and from the brainstem and cerebellum with a caudal coronal cut. In animals that were perfused with RNAlater, this block of tissue was sectioned coronally at 7 μm for laser capture. In animals that were perfused with 4% formaldehyde this block of tissue was sectioned coronally at 25 μm for ICC.

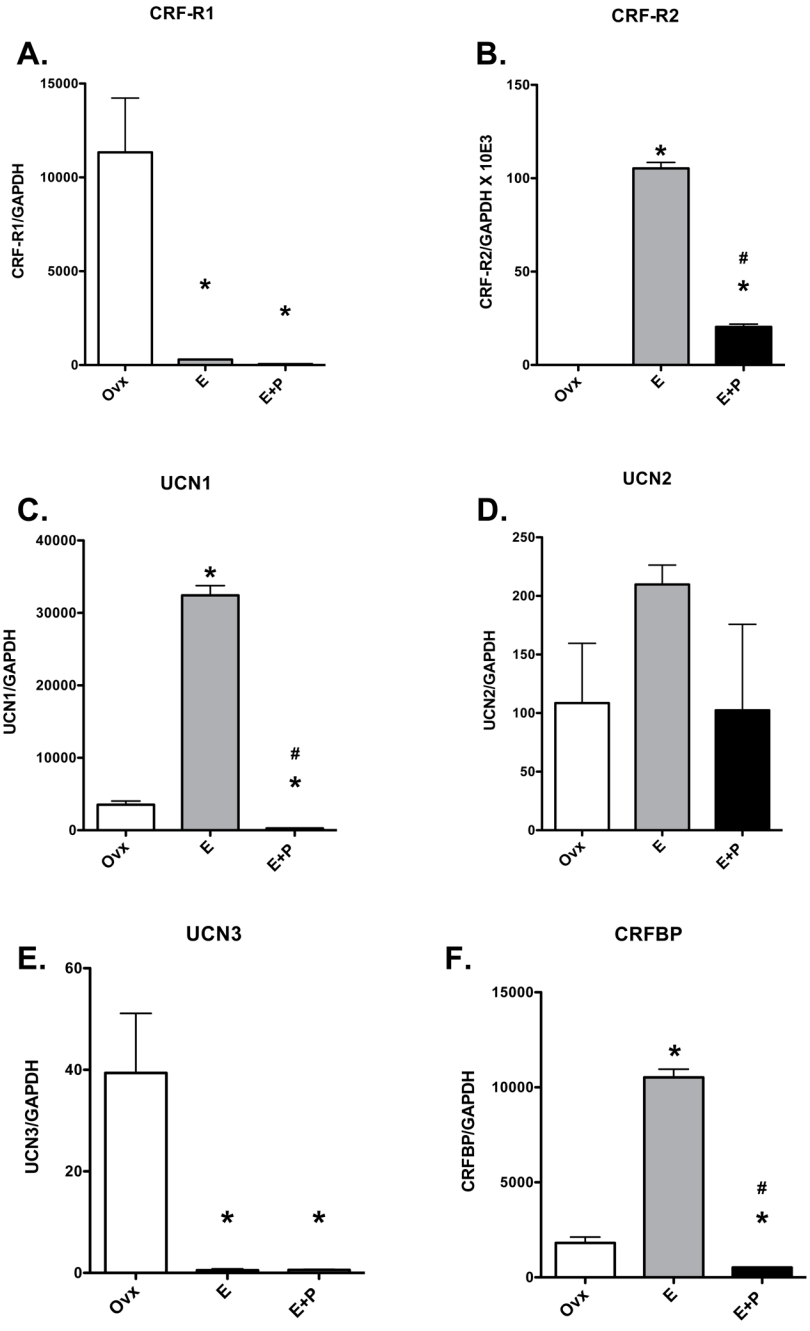

Figure 2.

Relative expression of stress-related genes in a hemi-midbrain block from ovariectomized monkeys treated with placebo (Ovx), estrogen (E) or estrogen +progesterone (E+P) for one month (n=4/group). Gene expression was determined with custom Taqman expression cards from ABI. Each transcript is normalized to GAPDH. **A.** The relative expression of CRF-R1 was significantly decreased by E and E+P treatments compared to the Ovx control group (ANOVA $p < 0.0014$). **B.** The relative expression of CRF-R2 was significantly increased by E treatment compared to the Ovx control group and then significantly reduced by P treatment. However, expression in the P group remained significantly higher than in the Ovx control group (ANOVA $p < 0.0001$). **C.** The relative expression of UCN1 was significantly

increased by E treatment compared to the Ovx control group and then significantly reduced by P treatment (ANOVA $p < 0.0001$). **D.** The relative expression of UCN2 was not affected by ovarian steroids. **E.** The relative expression of UCN3 was significantly reduced by E and E+P treatment compared to the Ovx control group (ANOVA $p < 0.0029$). However, the expression was at the limit of detection of the assay. **F.** The relative expression of CRFBP was significantly increased by E treatment compared to the Ovx control group and then suppressed by supplemental P treatment (ANOVA $p < 0.0001$). Asterisks (*****) mean $p < 0.05$ compared to Ovx control group and crosshairs (#) mean $p < 0.05$ compared to E group, Student-Newman-Keuls posthoc pairwise analysis.

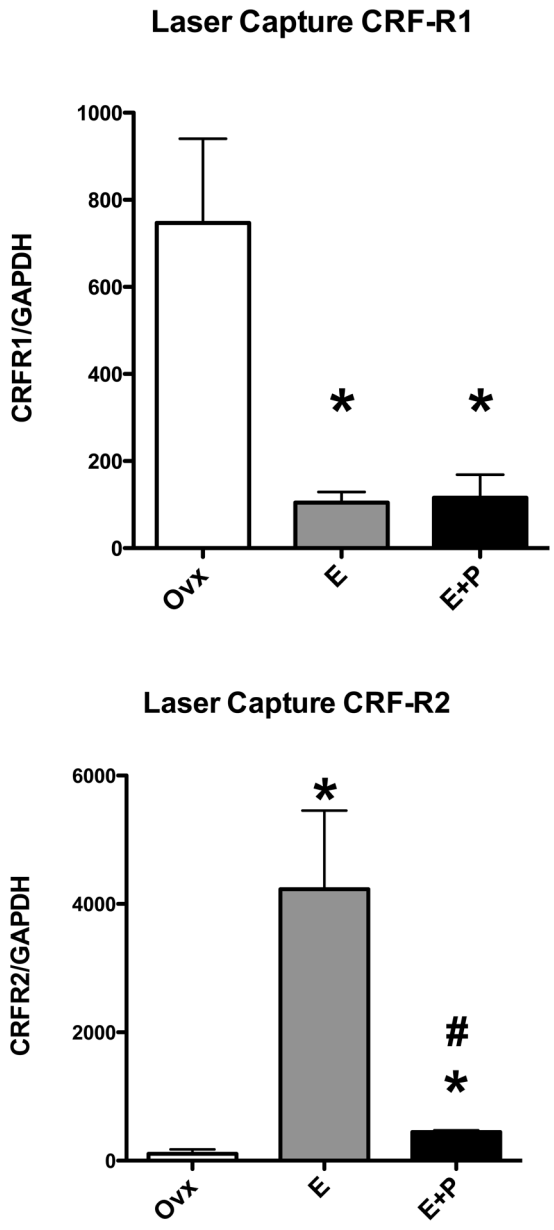

Figure 3.

Relative expression of CRF-R1 and CRF-R2 in laser captured serotonin neurons from ovariectomized monkeys treated with placebo (Ovx), estrogen (E) or estrogen +progesterone (E+P) for one month (n=3/group). Gene expression was determined with custom Taqman expression cards from ABI after amplification with a mix of primers. Each transcript is normalized to GAPDH. **Top.** The relative expression of CRF-R1 was significantly decreased by E and E+P treatments compared to the Ovx control group (ANOVA $p < 0.0124$). **Bottom.** The relative expression of CRF-R2 was significantly increased by E treatment compared to the Ovx control group and then significantly reduced by supplemental P treatment (ANOVA $p < 0.0044$). Symbols are as described in Figure 2.

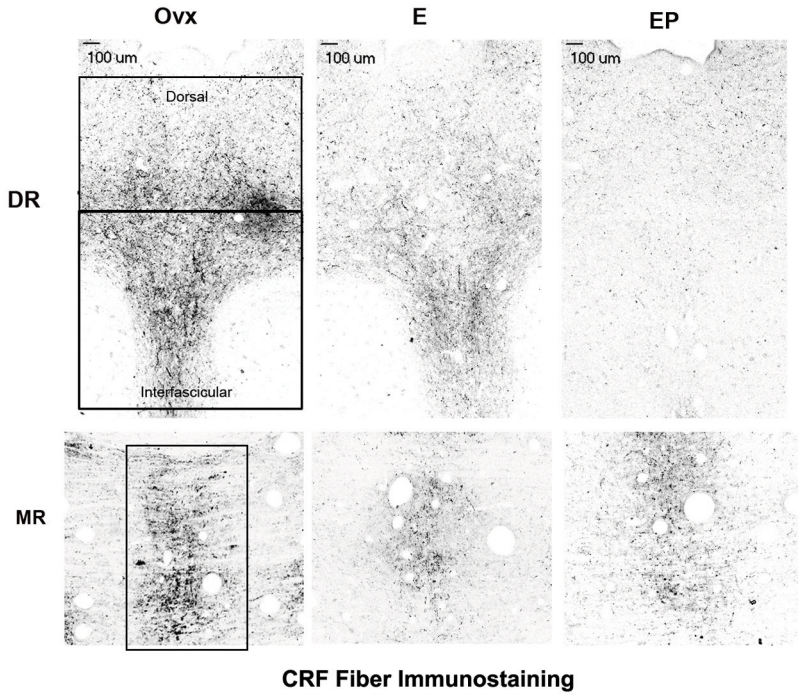

Figure 4.

Representative stereological montages of CRF-positive fibers in the dorsal (DR) and median (MR) raphe nuclei from ovariectomized monkeys treated with placebo (Ovx), estrogen (E) or estrogen +progesterone (E+P) for one month (n=5/group). The boxes demarcate the regions of interest of the raphe that were analyzed at this level. In the dorsal raphe (DR), the top area was designated the dorsal aspect of the dorsal raphe nucleus and the lower area was designated the interfascicular dorsal raphe nucleus. The size of the region of interest varied at each anatomical level, but it was always held constant across all animals. There is an apparent decrease in CRF-positive fibers in the animals treated with E or E+P compared to the Ovx control group.

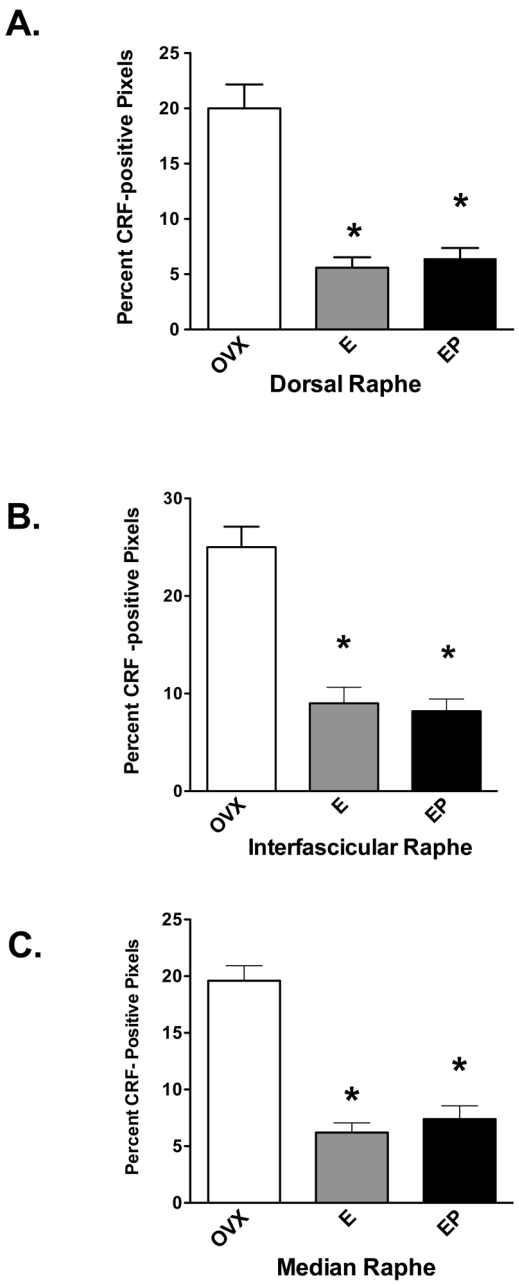

Figure 5.

Histograms representing the percent of CRF-positive pixels within the dorsal, interfascicular and median raphe nuclei from ovariectomized monkeys treated with placebo (Ovx), estrogen (E) or estrogen + progesterone (E+P) for one month (n=5/group). **A.** E and E+P significantly decreased the percent of CRF-positive pixels in the dorsal segment of the dorsal raphe nucleus in all four levels analyzed (ANOVAs range $p < 0.0001$ to 0.0006; not shown). When all levels were combined, E and E+P significantly decreased the mean percent of CRF-positive pixels compared to Ovx placebo-treated controls (ANOVA, $p<0.0001$). **B.** E and E +P significantly decreased the percent of CRF-positive pixels in the interfascicular segment of the dorsal raphe nucleus in all four levels analyzed (ANOVAs range $p < 0.0001$ to 0.02; not shown). When the interfascicular levels of the dorsal raphe nucleus were combined, E

and E+P significantly decreased the mean percent of CRF-positive pixels compared to Ovx placebo-treated controls (ANOVA, $p<0.0001$). **C.** E and E+P significantly decreased the percent of CRF-positive pixels in the median raphe in all four levels analyzed (ANOVAs range $p < 0.0001$ to 0.02; not shown). When the levels were combined, E and E+P significantly decreased the percent of CRF-positive pixels compared to Ovx placebo-treated controls (ANOVA, $p<0.05$). Symbols are as described in Figure 2.

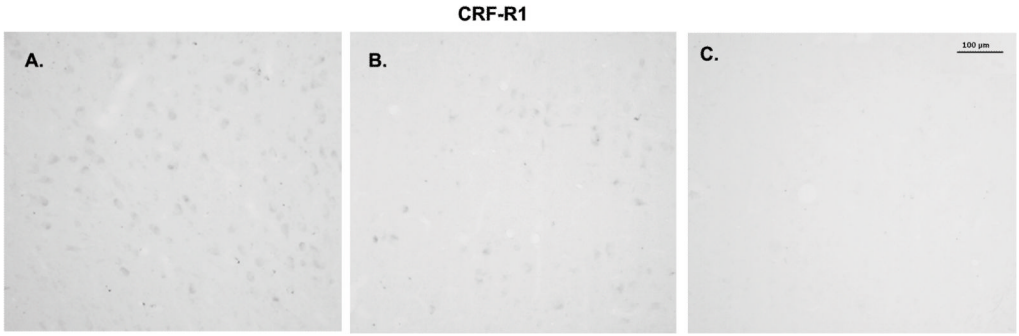

Figure 6.

Immunostaining of CRF-R1 in the dorsal raphe nucleus. **A.** Dorsal raphe nucleus from Ovx control animal immunostained with the CRF-R1 antibody diluted 1/500 in buffer. **B.** Dorsal raphe nucleus from Ovx control animal immunostained with the CRF-R1 antibody diluted 1/2000 in buffer. This was the highest dilution to produce immunostaining. **C.** Raphe section from the same animal incubated with the 1/2000 dilution of the primary antibody preabsorbed with 500 μg CRF-R1 peptide for 24 hours before incubation with the tissue section.

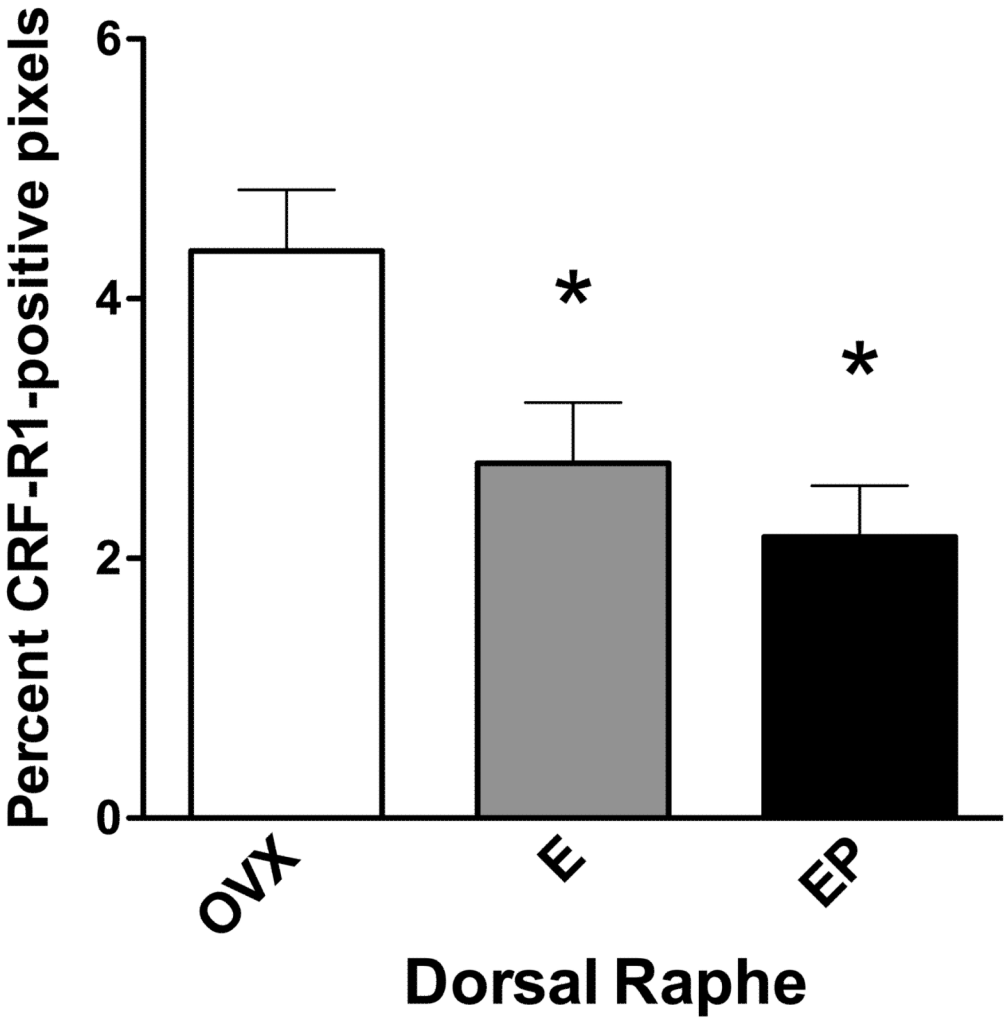

Figure 7.

Histogram representing the percent of CRF-R1-positive pixels within the dorsal raphe nucleus from ovariectomized monkeys treated with placebo (Ovx), estrogen (E) or estrogen +progesterone (E+P) for one month (n=3/group). A total of 5 levels at 500 μm intervals were examined. E and E + P significantly decreased the percent of CRF-R1-positive pixels in the third level of the dorsal raphe nucleus (ANOVA, $p < 0.0025$; not shown). When all levels were combined, E and E+P significantly decreased the mean percent of CRF-R1-positive pixels compared to OVX placebo-treated controls (ANOVA, $p < 0.03$). Symbols are as described in Figure 2.

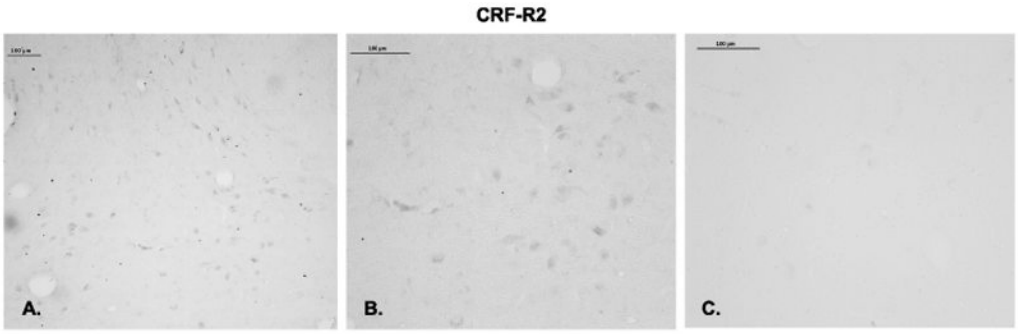

Figure 8.

Immunostaining for CRF-R2 in the ventral part of the dorsal raphe nucleus. **A.** Low power magnification of CRF-R2 immunostaining with a 1/750 dilution of the antibody. **B.** High magnification of CRF-R2 immunostaining with a 1/750 dilution of the antibody. **C.** Raphe section from the same animal incubated with 1/750 dilution of the primary antibody preabsorbed with 1 mg CRF-R2 peptide for 24 hours before incubation with the tissue section.

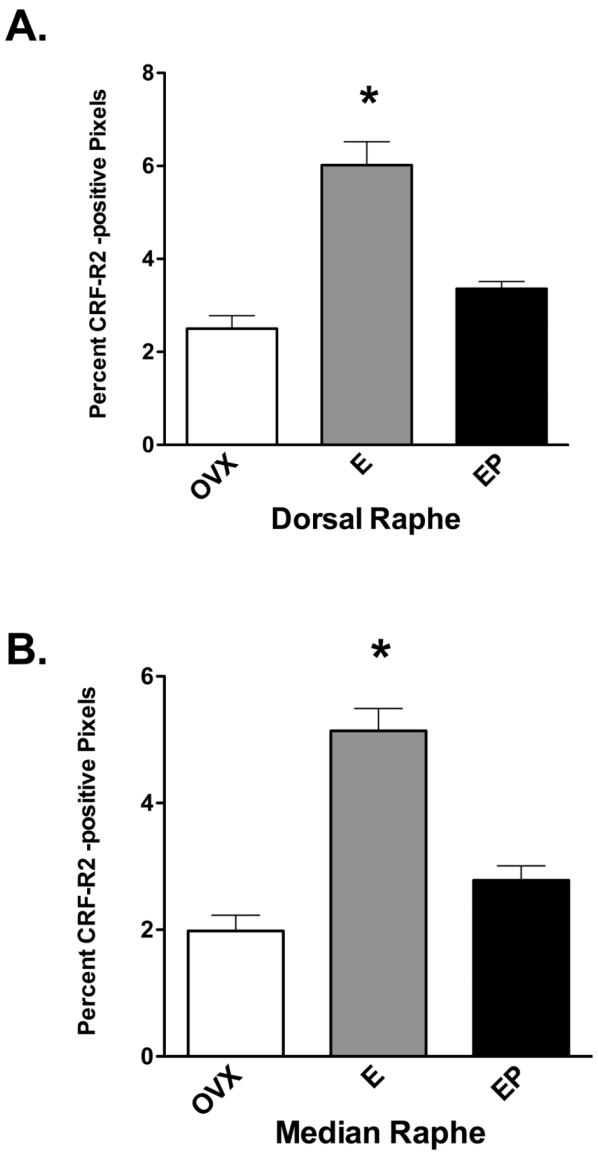

Figure 9.

Histograms representing the percent of CRF-R2-positive pixels in the dorsal and median raphe nuclei from ovariectomized monkeys treated with placebo (Ovx), estrogen (E) or estrogen +progesterone (E+P) for one month (n=5/group). **A.** The E-treated group showed a significantly higher percent of CRF-R2-positive pixels in the dorsal raphe nucleus compared to Ovx placebo- or E+P-treated groups in 4 of 5 levels examined (ANOVAs range $p < 0.0001$ to 0.014; not shown). When all 5 levels were combined, E and E+P significantly increased the mean percent of CRF-R2-positive pixels compared to Ovx placebo-treated controls (ANOVA, $p<0.05$). **B.** The E-treated group showed a significantly higher percent of CRF-R2-positive pixels in the median raphe nucleus compared to Ovx placebo- or E+P-treated groups at all 3 levels examined (ANOVAs range $p < 0.0001$ to 0.018; not shown). When all 3 levels were combined, E treatment significantly increased the mean percent of CRF-R2-positive pixels compared to Ovx placebo-treated controls (ANOVA, $p<0.0001$). Symbols are as described in Figure 2.

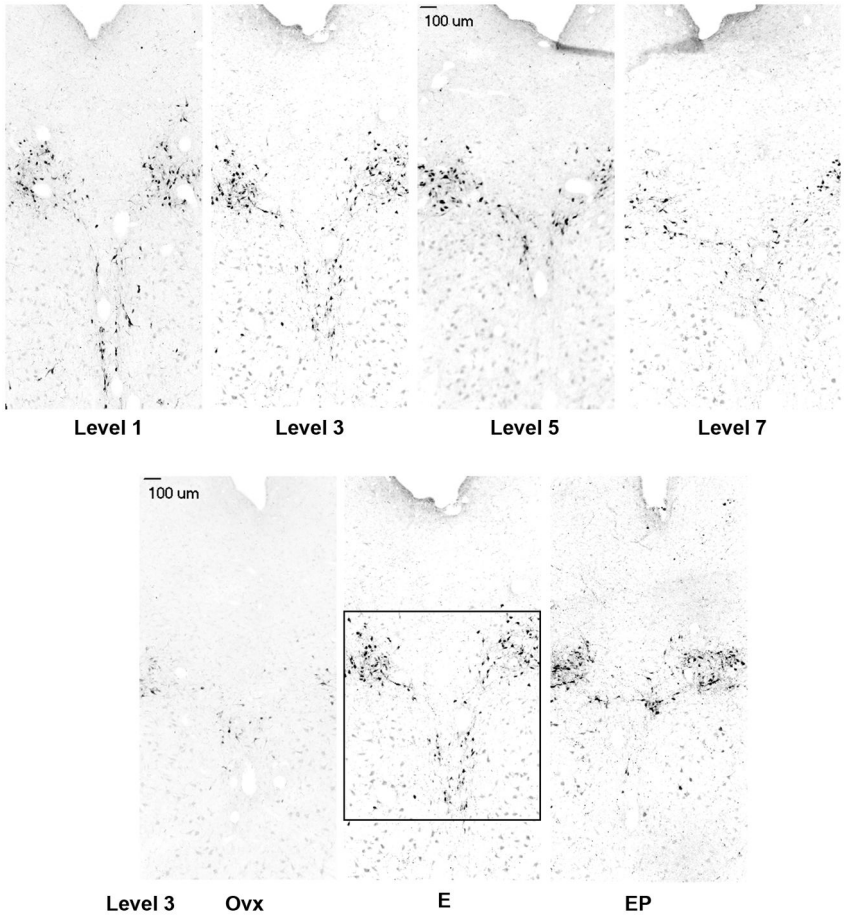

Figure 10.

Montages of UCN1 immunostained neurons in the supraoculomotor area (SOA) adjacent to the Edinger Westfal nucleus. **Top panels.** UCN1 immunostaining in representative sections of the SOA at 4 of the 8 levels that were subjected to quantitative analysis. Each level is 500 μm apart from a rostral to caudal direction. **Bottom panels.** UCN1 immunostaining in representative sections of the SOA from an ovx control, an E-treated and an E+P treated animal. There appears to be an increase in UCN1 cell staining with E and E+P treatment. The box demarcates the region of interest that was analyzed at level 3. The size of the region of interest varied at each anatomical level, but it was always held constant across all animals.

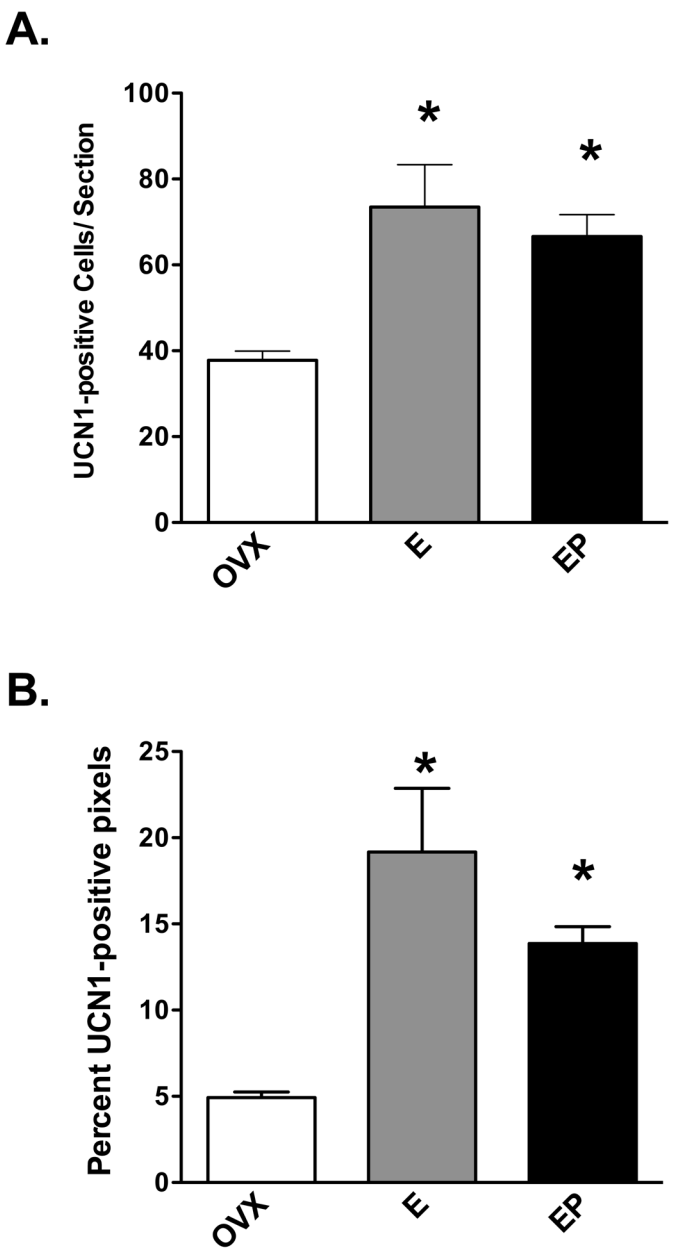

Figure 11.

Histograms representing the number of UCN1-positive neurons and percent UCN1-positive pixels within the supraoculomotor region in each treatment group (n=5/group). **A.** E or E+P significantly increased the number of UCN1-positive neurons in 7 of 8 levels analyzed (ANOVAs range $p < 0.0025$ to 0.038; not shown). When all 8 levels were combined, E and E+P significantly increased the mean number of UCN1-positive neurons per section compared to placebo-treated controls (ANOVA, $p<0.0029$). **B.** E and E+P also significantly increased the percent of UCN1-positive pixels in the supraoculomotor region in all 8 levels analyzed (ANOVAs range $p < 0.0001$ to 0.037; not shown). When the levels were combined, E and E+P significantly increased the mean percent of UCN1-positive pixels compared to placebo controls (ANOVA, $p<0.0001$). Symbols are as described in Figure 2.

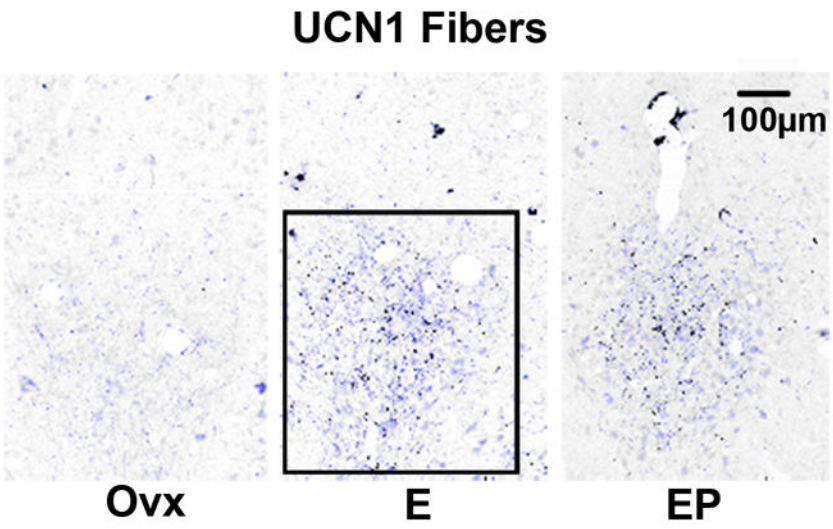

Figure 12.

Representative montages illustrating immunostaining for UCN1 fibers in the caudal linear nucleus from ovariectomized monkeys treated with placebo (Ovx), estrogen (E) or estrogen +progesterone (E+P) for one month (n=5/group). The UCN1 immunostained fibers have been segmented from background in blue. The box demarcates the region of interest that was analyzed at this level. The size of the region of interest varied at each anatomical level, but it was always held constant across all animals.

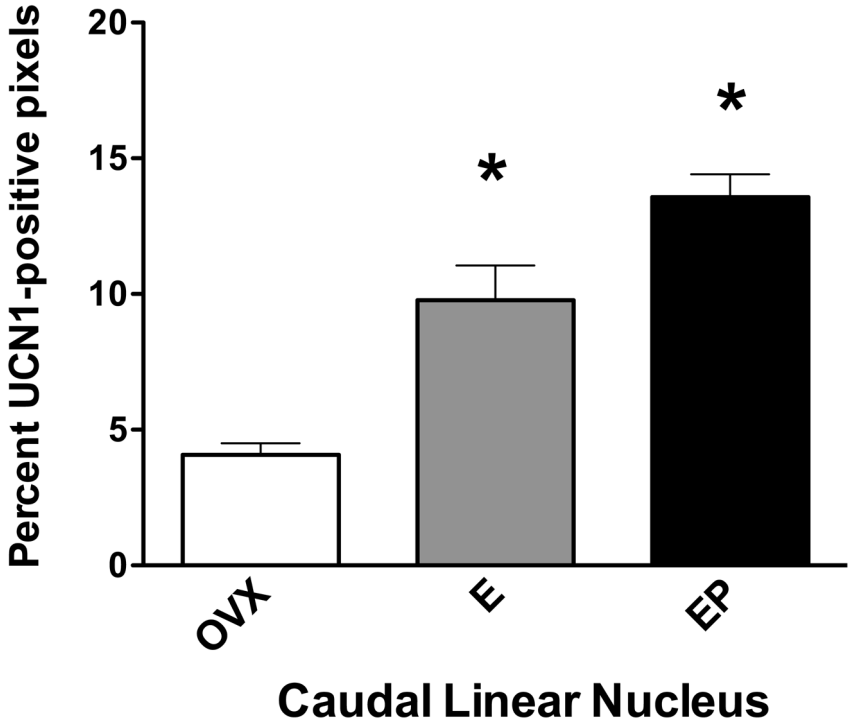

Figure 13.

Histogram representing the percent of UCN1-positive pixels in the caudal linear nucleus from ovariectomized monkeys treated with placebo (Ovx), estrogen (E) or estrogen +progesterone (E+P) for one month (n=5/group). E or E+P significantly increased the percent of CRF-positive pixels in the caudal linear raphe nucleus at all 3 levels examined (ANOVAs range $p < 0.0034$ to 0.0097; not shown). When all 3 levels were combined, E and E+P significantly increased the percent of UCN1-positive pixels compared to Ovx placebo-treated controls (ANOVA, $p<0.0001$). Symbols are as described in Figure 2.

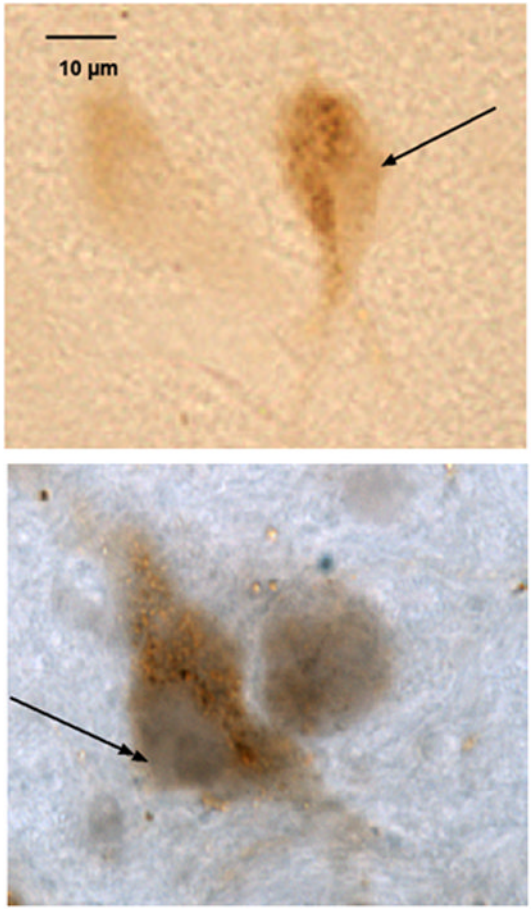

Figure 14.
Neurons in the supraoculomotor region of an E+P treated animal immunostained with antibodies against human UCN1 and nuclear estrogen receptor beta (ERβ). **Top.** Neuron immunostained for UCN1 only, visualized as a reddish-brown precipitate in the cytoplasm. There is no staining in the nucleus (single head arrow). **Bottom.** Neuron immunostained for UCN1 and ERβ. The immunostaining for ERβ appears purple and fills the nucleus (double headed arrow), while the reddish-brown precipitate for UCN1 fills the neuronal cytoplasm.

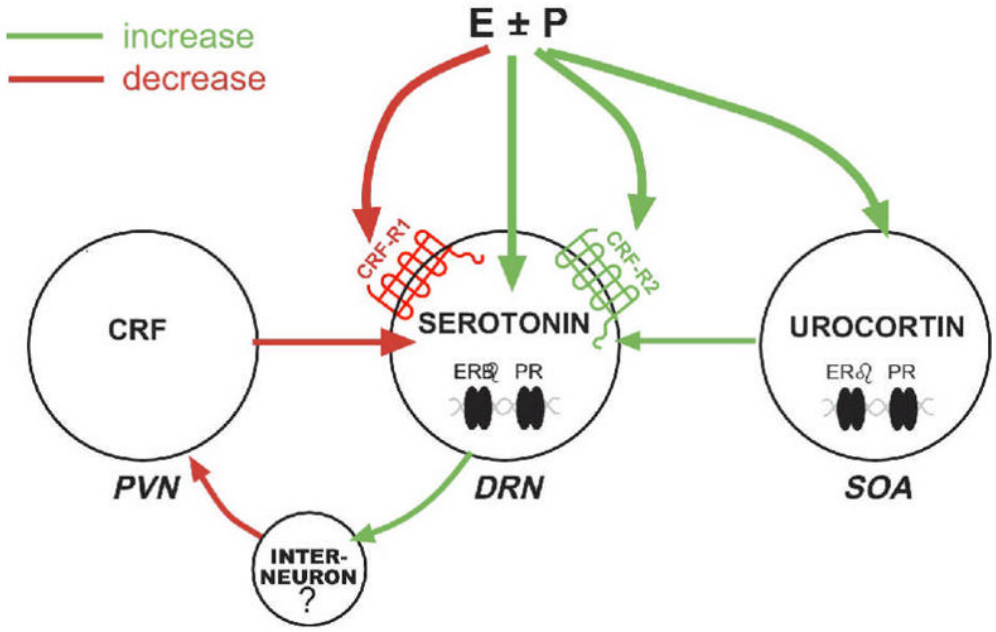

Figure 15.

A diagram of the hypothesized interactions of ovarian hormones and midbrain stress systems. We show herein that E±P decrease CRF innervation of the dorsal and median raphe nuclei, the location of serotonin cell bodies that project to the forebrain. In addition, E±P decrease CRF-R1 and increase CRF-R2 on serotonin neurons. We also show that E±P increases UCN1 production and fiber density rostral to the dorsal raphe, and those UCN1 neurons contain ERβ. PR is also likely present in UCN1 neurons that colocalize CART (Lima et al., 2008). We have previously shown that serotonin neurons contain ERβ and PR, which in turn increase production of serotonin (Bethea, 1993, 1994, Gundlah et al., 2001). We speculate that serotonin projects to the hypothalamus and stimulates an inhibitory interneuron that inhibits CRF production in the PVN (Bethea and Centeno, 2008). This does not rule out a direct action of E±P on CRF in the PVN, but an inhibitory effect has not been observed in molecular studies.

Table 1

Available information about ABI custom Taqman qPCR assays.

Gene Name	Gene Symbol	Assay ID	Context Sequence	NCBI Gene Reference
urocortin 1	UCN1	Rh03986716_s1	GCCGAGCAGAACCGCATCATATTCG	XM_001092424.1,XM_001092536.1
urocortin 2 preproprotein	UCN2	Rh02822047_m1	AGAAGAAGCTGGTGGCGCCTGACCT	XM_001097967.1
urocortin 3 (stresscopin)	UCN3	Rh03986721_m1	GTCCACTCTCAGGGAGAGATGCCGA	XM_001104616.1
corticotropin releasing factor receptor type 1	CRFR1	Rh02787591_m1	GACAATGAGAAGTGCTGGTTTGGCA	NM_001032803.1,AB078141.1
corticotropin releasing hormone receptor 2	CRFR2 (LOC697404)	Rh01120857_m1	AGTACAACACGACCCGGAATGCCTA	XM_001085987.1
corticotropin releasing hormone binding protein	CRHBP	Rh01075813_m1	GGGCGGCGACTTCCTGAAGGTATTT	XM_001106453.1,XM_001106396.1
tryptophan hydroxylase 2	TPH2	Rh02788839_m1	CTACTCGGCAACTTAACACTAAATA	NM_001039946.1,AY827483.1,DQ360113.1